



# Search for GeV gamma rays & Dark Matter Annihilation to gamma-rays from SPT-SZ selected Galaxy Clusters



17th International Conference on Interconnections between Particle Physics and Cosmology (PPC 2024)

Siddhant Manna & Shantanu Desai  
IIT Hyderabad

---

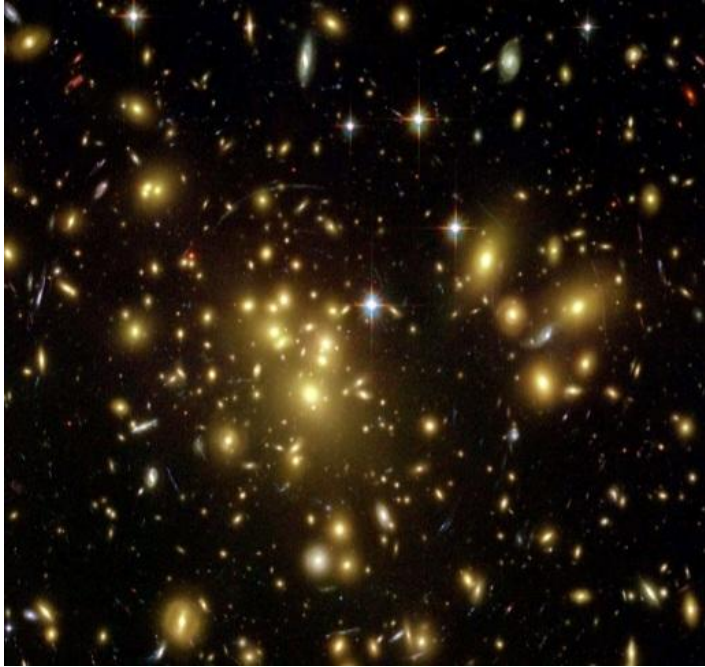
# Our Publications

---

1. Search for GeV Gamma-Ray Emission from SPT-SZ selected Galaxy Clusters with 15 years of Fermi-LAT data, published in [JCAP](#). 
2. Search for Dark Matter Annihilation to gamma-rays from SPT-SZ selected Galaxy Clusters. Published in [JCAP](#). 
3. A pilot search for MeV gamma-ray emission from five galaxy clusters using archival COMPTEL data. Published in [JCAP](#).
4. Search for GeV gamma-ray emission from SPT-CL J2012-5649 with six years of DAMPE data. Published in [JHEAP](#).

Today's Talk

# Galaxy Clusters



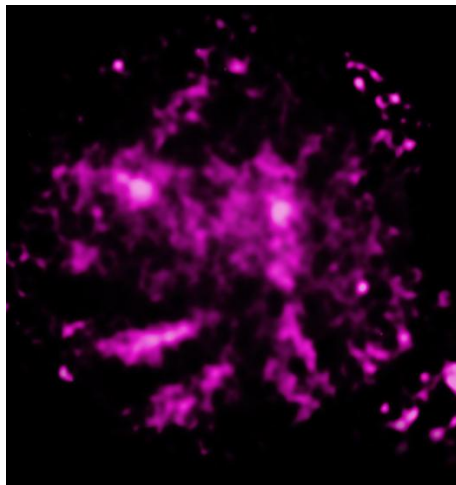
**Abell 1689**

**Credit: N.Benitez (Hubble Space Telescope)**

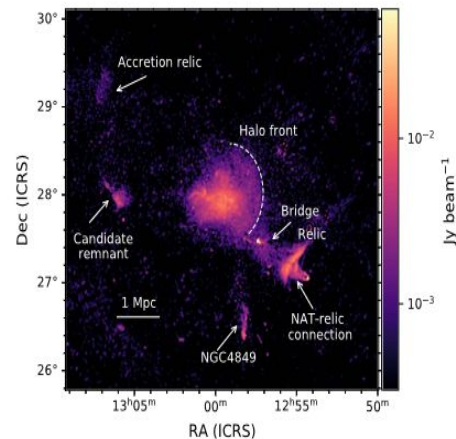
- ★ Most massive gravitationally collapsed objects with masses  $> 10^{14} M_{\odot}$ . It's typical size is of 1-10 Mpc.
- ★ Composed of nearly **2% galaxies, 13% Plasma (Baryons) and 85% Dark Matter.**



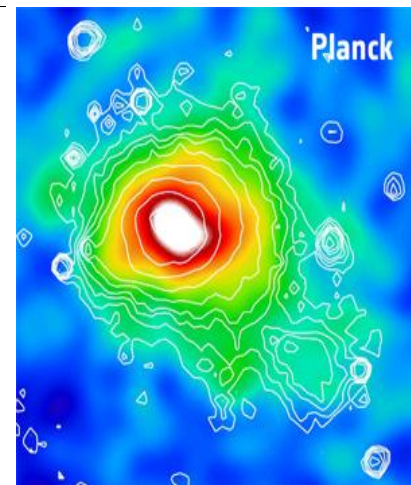
Coma Cluster in Optical data from SDSS  
Credits: [Chandra X ray](#)



Coma Cluster in X-ray data from NASA's Chandra X-ray Observatory and ESA's XMM-Newton.  
Credits: [Chandra X ray](#)



Radio image of the Coma cluster.  
Credits: [arXiv 2203.01958](#)



Coma cluster as seen by Planck through the SZ effect.  
Credits: [Planck Mission](#)

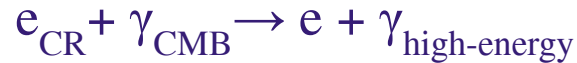
**Still, Detection of galaxy clusters in gamma rays (> MeV energies) is still an open question.**

# How are gamma rays produced

1. Interactions of CR protons with interstellar nuclei produce  $\gamma$  rays through decay of neutral pions.



2. Cosmic ray electrons scatter off low-energy photons (CMB), boosting the photon energy to gamma-ray levels. (Inverse Compton scattering).



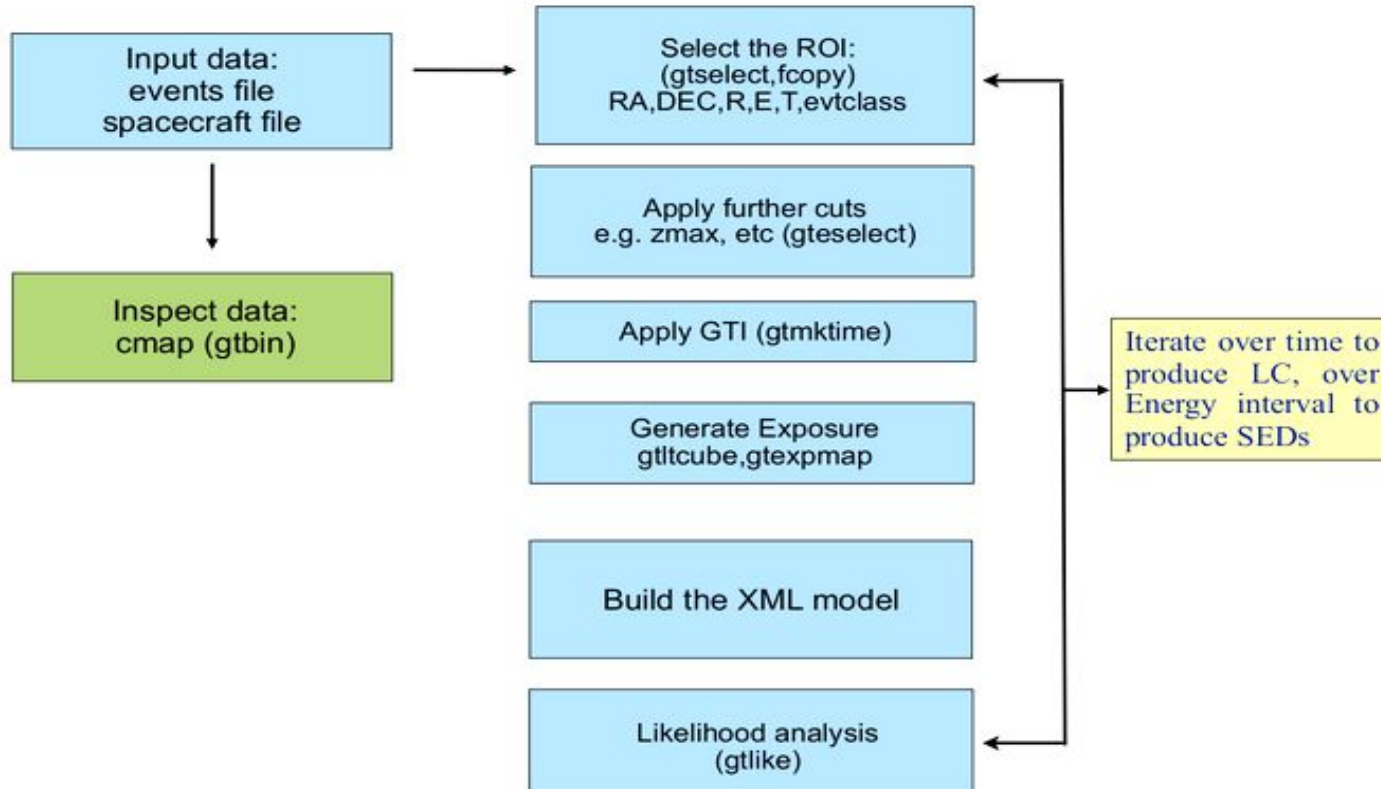
**OR, Through DARK MATTER Annihilation or decay as we will see later.**

# What is Fermi Gamma-Ray Space Telescope?

- NASA's Fermi Gamma-ray Space Telescope is a powerful space observatory that detects gamma rays, and was launched in 2008.
- It carries two scientific instruments, pictured at right: the Large Area Telescope (LAT) and the Gamma-ray Burst Monitor (GBM). LAT works in the energy range from 20 MeV to 300 GeV.
- Due to the large Point Spread Function (PSF) at lower energies, we avoided analyzing data below 1 GeV. At the lowest energy considered of 1 GeV, the PSF is around  $1.72^\circ$  and for the highest energy considered of 300 GeV, the PSF is found to be  $0.17^\circ$ .



## Schematic view of the process



# Maximum Likelihood Analysis (MATTOX 1996)

Likelihood Function is given as:

$$L(\vec{\theta}) = \prod_{ij} \frac{\theta_{ij}^{n_{ij}} e^{-\theta_{ij}}}{n_{ij}!}$$

OR

Log-Likelihood Function :

$$\ln L(\vec{\theta}) = \sum_{ij} n_{ij} \ln \theta_{ij} - \sum_{ij} \theta_{ij}$$

$$TS = 2 \times (\ln L - \ln L_0)$$





# South Pole Telescope Cluster Catalog (SPT-SZ)

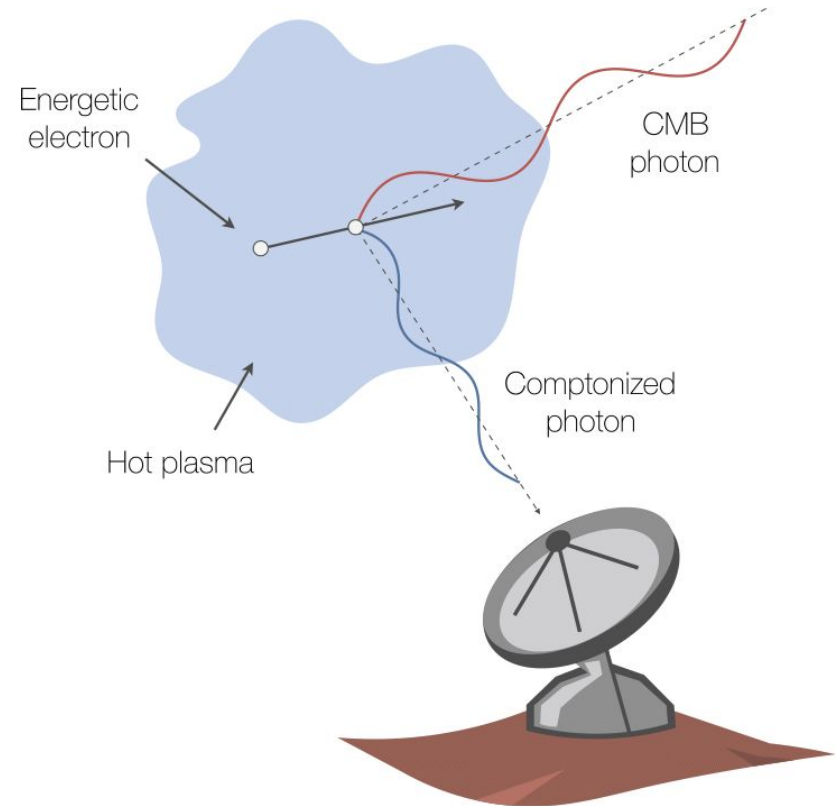
- ★ It is a 10-meter diameter microwave / millimeter / submillimeter wavelength telescope located at the NSF Amundsen-Scott South Pole Station and has an angular resolution of approximately 1 arcminute.
- ★ SPT completed a 2500 square-degree survey between 2007 and 2011 to detect galaxy clusters using the **SZ effect**.
- ★ **Important to note that SPT-SZ 2500d is a mass limited catalog as SZ effect is only a redshift distortion and flux does not scale as  $1/r^2$ .**
- ★ This survey detected **677 confirmed galaxy clusters** with SNR greater than 4.5, corresponding to a mass threshold of  $3 \times 10^{14} M_{\odot}$  up to **redshift of 1.8**



CREDITS: [SOUTH POLE TELESCOPE](#)

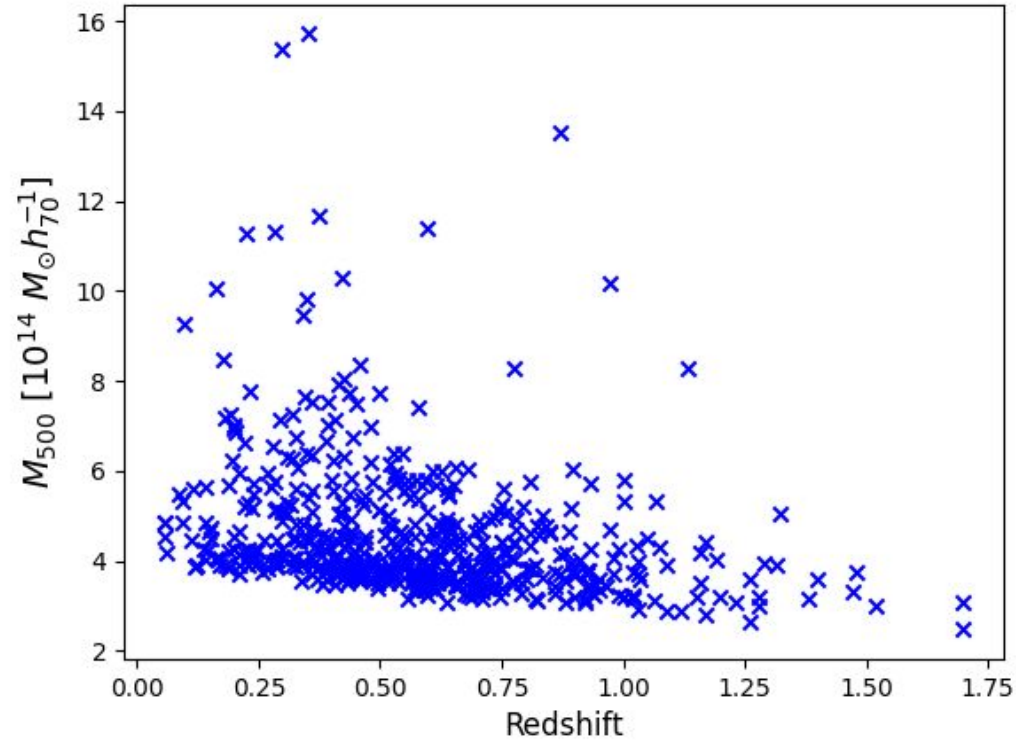
# Sunyaev-Zel'dovich effect (SZE)

- ★ **Sunyaev-Zel'dovich effect (SZE)** is a small spectral distortion of the cosmic microwave background (CMB) spectrum caused by the scattering of the CMB photons off a distribution of high energy electrons.
- ★ **Thermal SZE** is caused by the hot thermal distribution of electrons provided by the intra-cluster medium (ICM) of galaxy clusters.
- ★ As shown in the right, a **CMB photon (red)** enters the **hot ICM (light blue)** from an arbitrary angle, and on average is up-scattered to **higher energy (blue)** by an **electron (black)**.

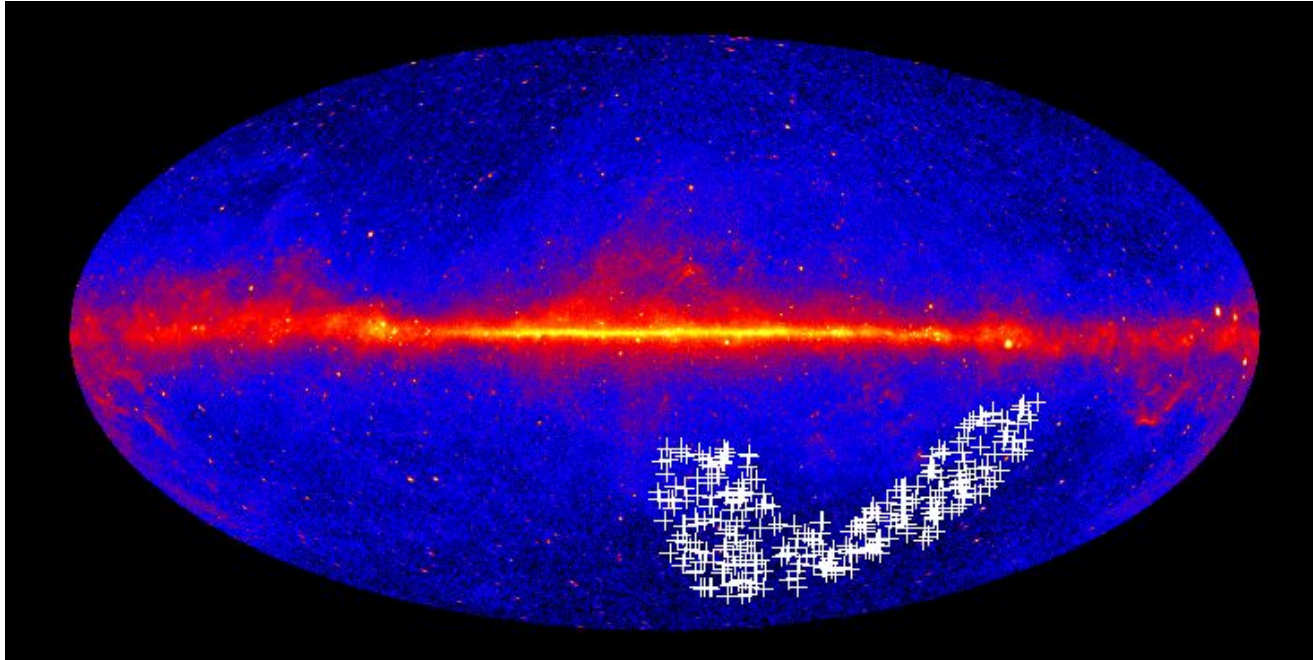




# Plot showing distribution of Mass with redshift

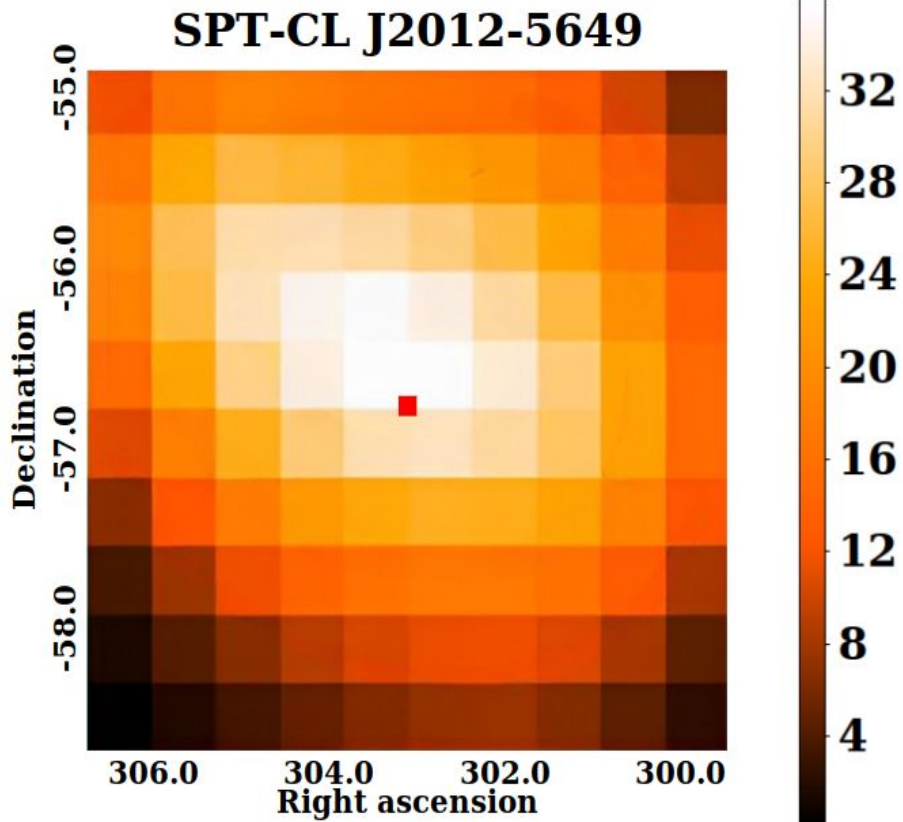


# Galaxy clusters we studied



The white colored plus sign depicts the locations of the 300 SPT-SZ galaxy clusters we used in our analysis. The bright, diffuse glow running along the middle of the map, shows the central plane of our Milky Way.

But, Within  $0.2^\circ$ ,  
we found six  
SUMSS radio  
sources

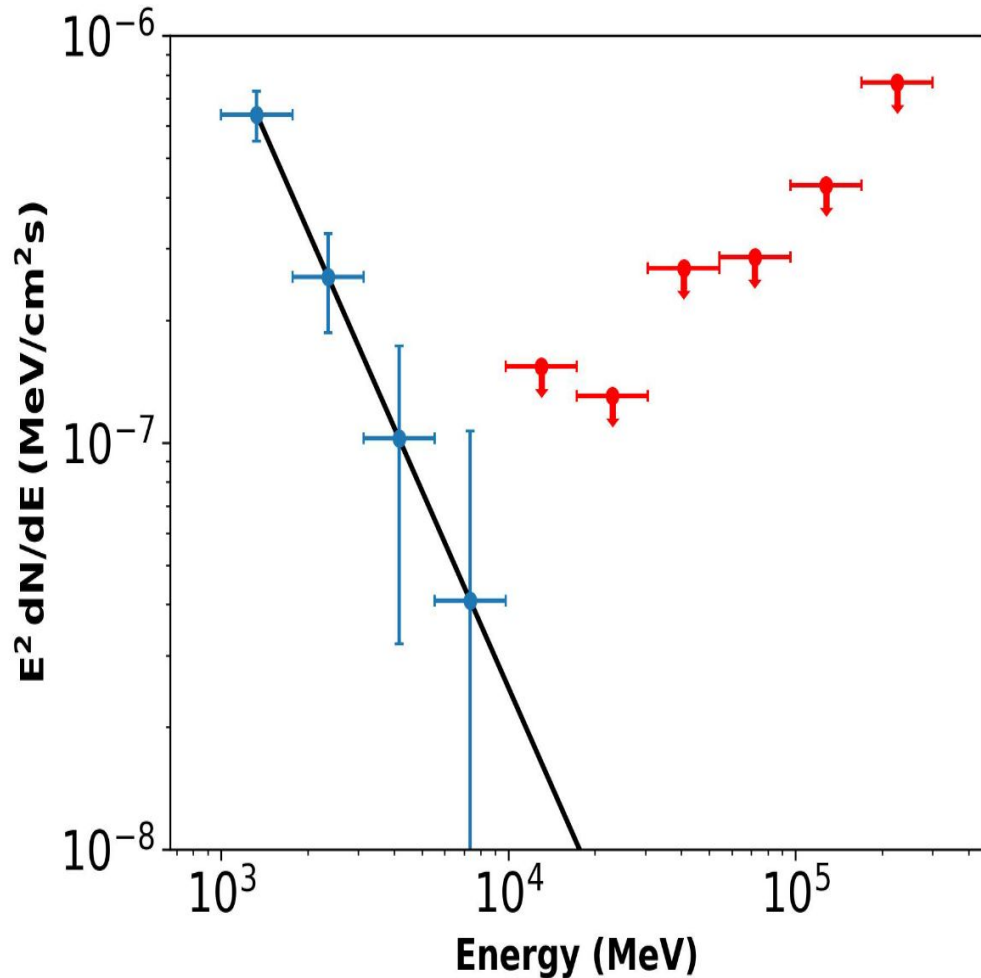


$6.1\sigma$   
detection

WOAH!!!

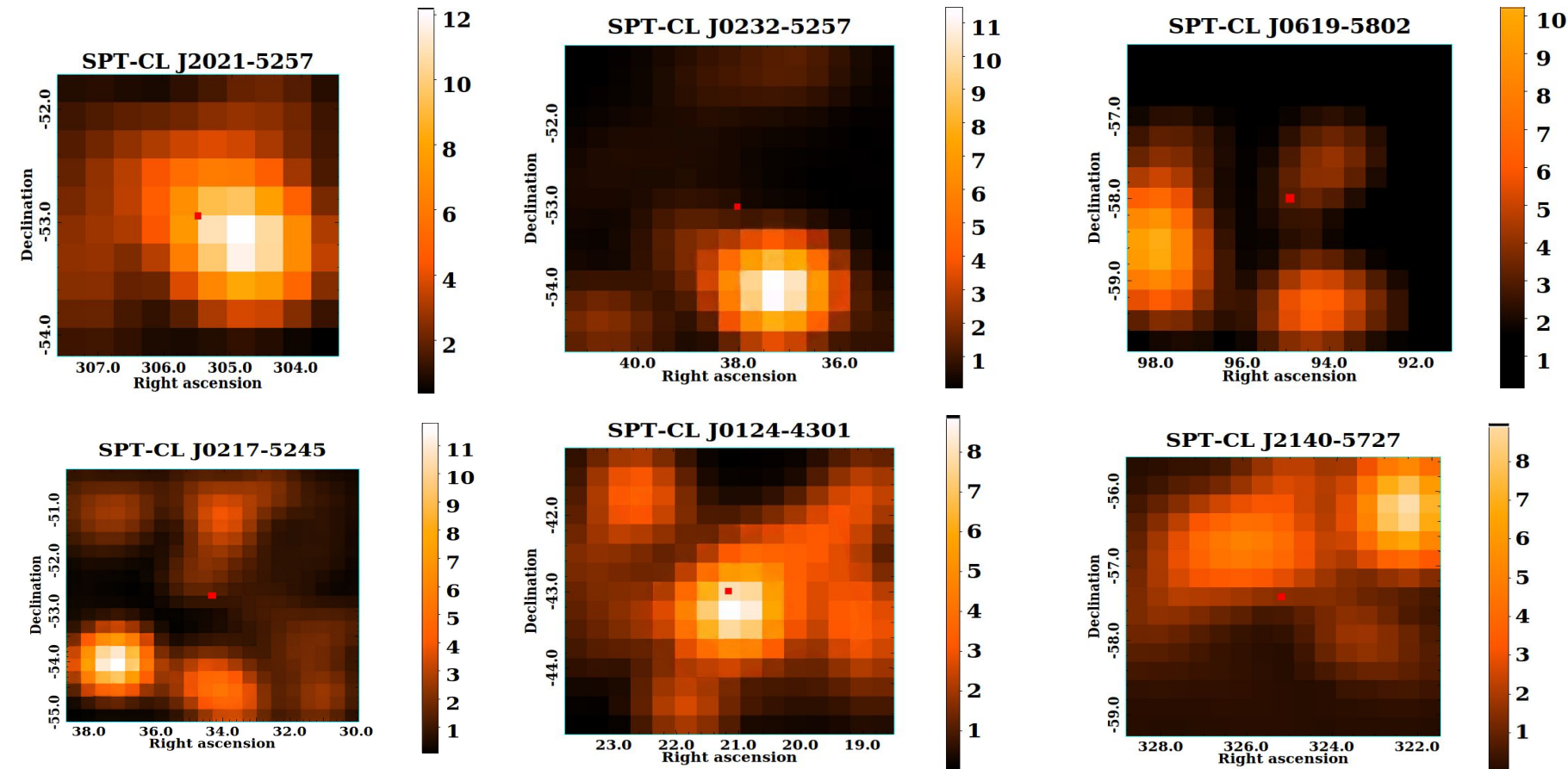


TS map for SPT-CL J2012-5649 (Abell  
3667) with significance  $> 5\sigma$

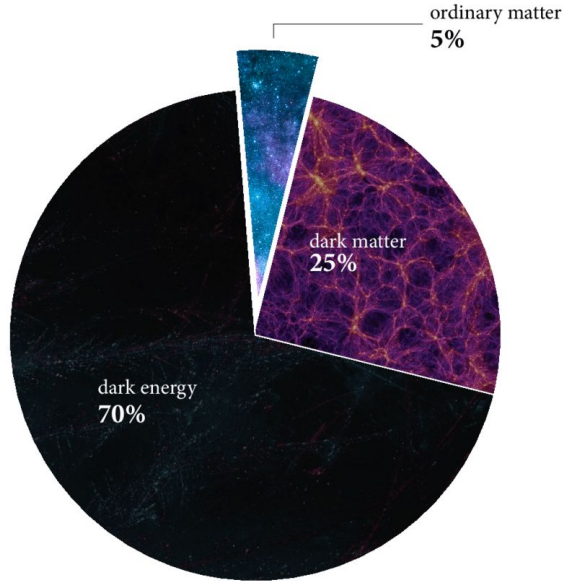


- ★ The differential energy spectrum from SPT-CL J2012-5649 obtained using easyFermi.
- ★ The solid line shows the power-law fit with the best-fit spectral index given by  $\gamma = -3.61 \pm 0.329$ .
- ★ The blue data points show the measured differential energy spectrum, while the red point represent upper limits. All the signal is observed at energies  $\leq 10$  GeV, and beyond that we obtain upper limits

# TS maps of galaxy clusters $3\sigma < \text{significance} < 5\sigma$



# Dark Matter Analysis



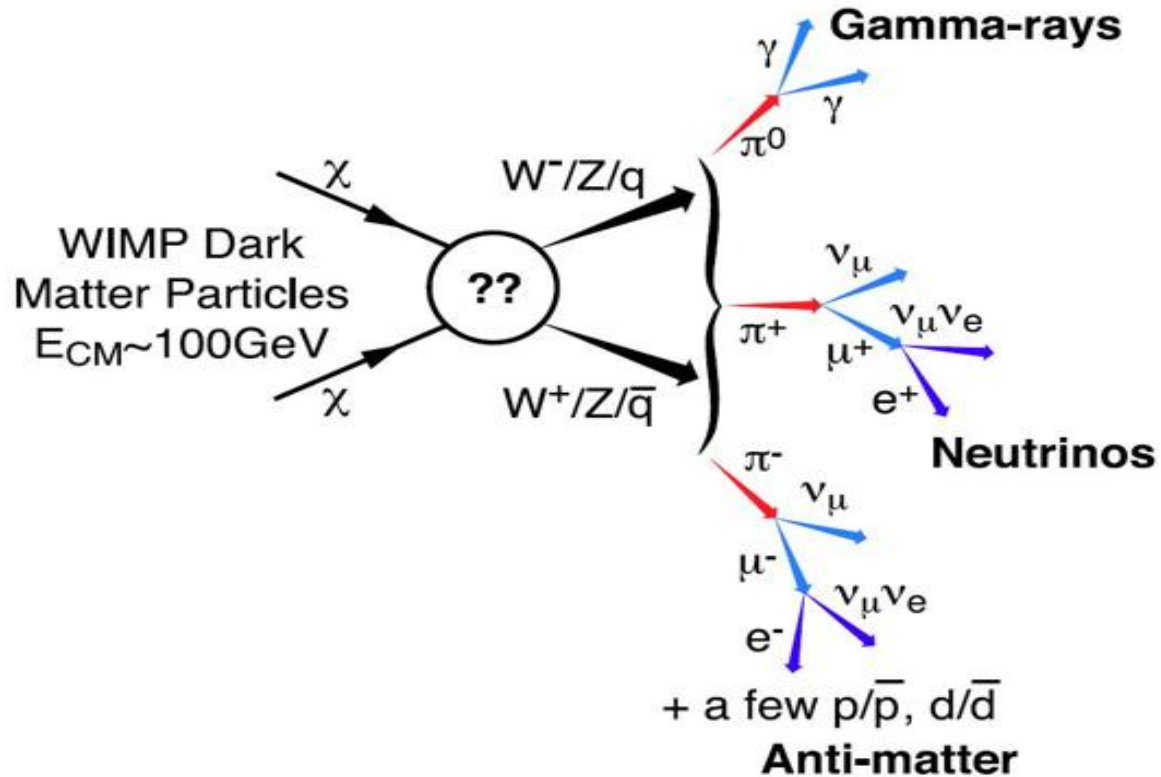
Energy content of the Universe according to the Standard Model

[Reference](#)

- About 80% of the mass in a cluster is in the form of dark matter, which holds everything else together.
- One of the most well motivated and widely studied dark matter candidate is a **weakly interacting massive particle (WIMP)**, which is a hypothetical stable particle, assumed to be a Majorana fermion with masses in the GeV-TeV range.
- We look for signatures of **WIMP annihilation** into secondary particles such as gamma-rays using galaxy clusters for a sample of 350 galaxy clusters from the SPT-SZ 2500d square catalog. The clusters are ranked in decreasing order of their mass ratio,  $M^{500}/z^2$ .



# Dark matter annihilation to standard model particles



# Dark Matter Analysis

The expected **gamma-ray flux** from the annihilation of WIMPs can be computed as:

$$d\Phi_{\gamma}/dE (E, \Delta\Omega, \text{l.o.s}) = d\phi_{\gamma}/dE (E) \times J(\Delta\Omega, \text{l.o.s})$$

- $d\Phi_{\gamma}/dE$  is the **WIMP dark matter induced differential gamma-ray flux** per unit energy and solid angle as a function of energy (E), solid angle ( $\Delta\Omega$ ), and line of sight (l.o.s.).
- The term  $d\phi_{\gamma}/dE (E)$  is the **gamma-ray energy spectrum per annihilation** as a function of energy and represents the particle physics component of the gamma-ray flux, which encapsulates the spectral characteristics of the WIMP annihilation such as the properties of the dark matter particles and the annihilation channels involved.

**Differential gamma-ray flux** is then computed as:

$$d\phi_{\gamma}/dE (E) = \langle\sigma v\rangle/8\pi m_{\chi}^2 \times dN_{\gamma} (E)/dE$$

- Here,  $dN_{\gamma} (E)/dE$  denotes the **WIMP photon spectrum**. The mass of the WIMP, denoted as  $m_{\chi}$ , determines the energy scale of the gamma rays produced during annihilation. The thermally-averaged annihilation cross-section, represented by  $\langle\sigma v\rangle$ , quantifies the likelihood of dark matter particles annihilating when they encounter each other.

- We can define the astrophysical J-factor  $J(\Delta\Omega, \text{l.o.s.})$  as the line-of-sight integral of the squared DM density profile over the solid angle at a given coordinate in the l.o.s. directions. J-Factor is given as:

$$J(\Psi, \theta, \Delta\Omega) = \int_0^{\Delta\Omega} \int_{\text{l.o.s.}} dl d\Omega \times \rho_{\text{tot}}(r)^2$$

- Here,  $\Delta\Omega$  is the solid angle over which the integration is performed,  $\rho_{\text{tot}}(r)$  is the total dark matter density profile as a function of the distance  $r$  from the centre of the system, and the integration is carried out along the line-of-sight (l.o.s.). The solid angle  $\Delta\Omega$  is related to the integration angle  $\alpha_{\text{int}}$  as:

$$\Delta\Omega = 2\pi(1 - \cos \alpha_{\text{int}})$$

- where  $\alpha_{\text{int}}$  is the angle between the line-of-sight and the direction pointing toward the centre of the astrophysical system. In our study, the integration angle  $\alpha_{\text{int}}$  is considered as  $0.2^\circ$ .

# Main Halo Modelling

- In the context of modelling the dark matter distribution within galaxy clusters, a common approach is to consider the total dark matter density profile as the sum of two components:

$$\rho_{\text{tot}}(r) = \rho_{\text{main}}(r) + \langle \rho_{\text{subs}} \rangle(r)$$

- The first term on the right-hand side,  $\rho_{\text{main}}(r)$ , represents the smooth, large-scale distribution of dark matter within the main halo of the galaxy clusters, whereas the second term ( $\langle \rho_{\text{subs}} \rangle(r)$ ) accounts for the contribution of the population of subhalos within the main halo of the galaxy cluster, according to the standard  $\Lambda$ CDM cosmological model.
- We modelled the main smooth dark matter halo using the Navarro-Frenk-White (NFW) density profile as:

$$\rho(r) = \rho_0 / (r / r_s) (1 + r/r_s)^2$$

- $\rho_0$  is the characteristic dark matter density for the NFW profile and  $r_s$  is the NFW scale radius. The NFW profile is usually reparameterized in terms of the halo mass and concentrations.
- We use the c-M relation defined in [arXiv 1312.1729](https://arxiv.org/abs/1312.1729) by M. A. Sánchez-Conde and F. Prada, 2014, which have been shown to match the observation results across a wide range of halo masses, from dwarf spheroidal galaxies to galaxy cluster

# Modelling the subhalo

- Subhalos are smaller-scale dark matter structures that are gravitationally bound within the larger main halo. Galaxy clusters are expected to host a large number of subhalos.
- For this purpose, we use the software [CLUMPY v3](#), where the [Einasto profile](#) is used to describe the density distribution of subhalos. The distribution of subhalos within a main halo is influenced by both their distance from the host center and also their mass.
- The [total distribution of subhalos](#) can be expressed as the product of three uncorrelated probability distribution functions (PDFs) and a normalization factor as:

$$d^3N / dV dM dc = N_{\text{tot}} dP_v(R)/dV \times dP_M(M)/dM \times dP_c(M,c)/dc$$

- $N_{\text{tot}}$  refers to the expected number of subhalos within the virial radius of main halo, and  $P_i$  with  $i = V, M, c$  is the probability distribution in each of the respective domains, normalized to 1. Here,  $V$  corresponds to the volume of the main halo,  $M$  pertains to the distribution of subhalo masses, and  $c$  represents the subhalo concentration.

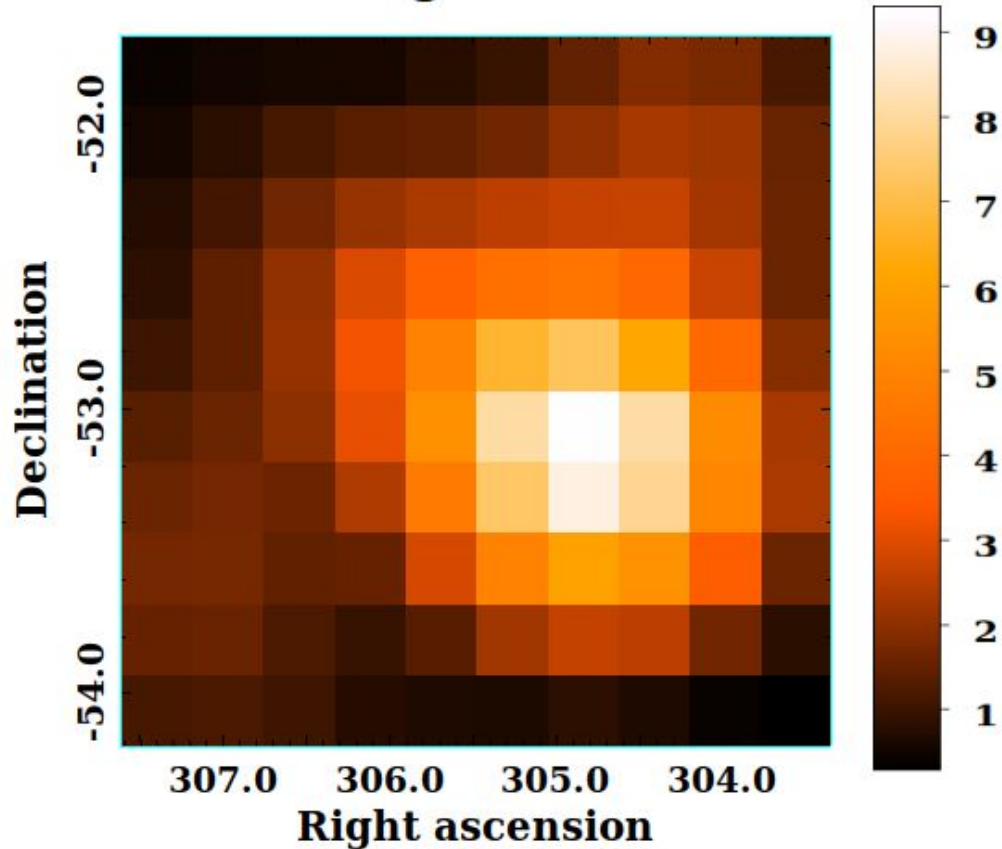
- Although, numerical cosmological simulations have significantly advance our understanding of halo substructures, **several questions still remain unresolved**, such as the **minimum mass for clump formation, the effects of tidal stripping on subhalo survival, and the exact shape of subhalo DM density profiles**. These uncertainties impact the calculation of the DM-induced  $\gamma$ -ray flux. To account for these, we used the following modelling:
- Spatial distribution PDF ( $dP_v(R)/dV$ ): Since the main halo is spherically symmetrical, the distribution of subhalos within it depends only on their distance from the central point of the host halo. We modelled it using the **Einasto profile**.
- Mass distribution PDF ( $dP_m(M)/dM$ ): **Subhalo mass function can be defined as:  $dP_M/dM \propto M^{-\alpha}$** . We have used  $\alpha = 1.9$  in our study similar to literature.
- Concentration distribution PDF ( $dP_c(M, c)/dc$ ): subhalos experience tidal forces that generally result in significant mass loss, particularly in their outer regions. As a result, subhalos tend to be more concentrated compared to the main halos with equivalent mass . **We have used  $(c - M)$  relation defined in [arXiv 1603.04057](#)** for the subhalos. It accounts for the spatial dependence of the subhalos within the main halos

# Analysis Process

---

- Our analysis followed the standard **binned-likelihood method for radius of  $10^\circ$  and energy range 1-300 GeV for 350 clusters** which are arranged according to  $M_{500}/z^2$  values.
- We incorporated sources from the 4FGL catalog up to  $10^\circ$  beyond the defined ROI into our model, freezing all their parameters to the catalog values. This was done to minimize bias from the potential presence of bright sources outside the targeted area and to account for the LAT's poor point spread function (PSF) at low energies around 1 GeV.
- Initially, the spectral parameters for all the free sources were determined. Then, we fixed the spectral parameters of all sources, except for the normalizations to their best-fit values and included a **template for potential dark matter annihilation emission in the model which we modelled as a diffuse source with a spatial distribution proportional to the J-factor calculated using CLUMPY.**
- The **spectral component** of the signal was given by the spectrum of annihilating dark matter for the specified channel utilizing the **DMFit Function** within Fermi tools by [arXiv 0808.2641](#).
- We used the gtapps tool for our analysis and employed the Maximum Likelihood Estimation (MLE) technique to identify the model parameters that best match the source's spectrum and location. The gtlike tool performs a binned likelihood analysis on Fermi-LAT gamma-ray data. Then we calculated Test Statistic values.

# SPT-CL J2021-5257



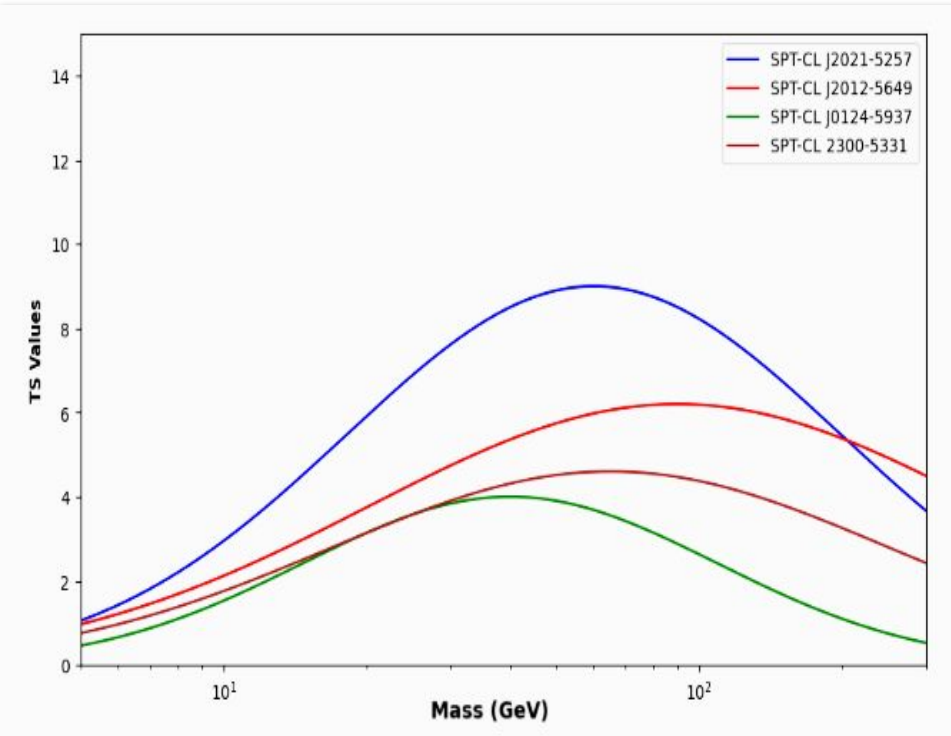
## TS Map

- Gaussian kernel smoothed ( $\sigma = 1.5$ ) TS map of the SPT-CL J2021-5257 cluster (left) and TS map scale (right) generated using gttsmap in the energy band 1 – 300 GeV.
- We used 0.2-pixel resolution for the spatial binning

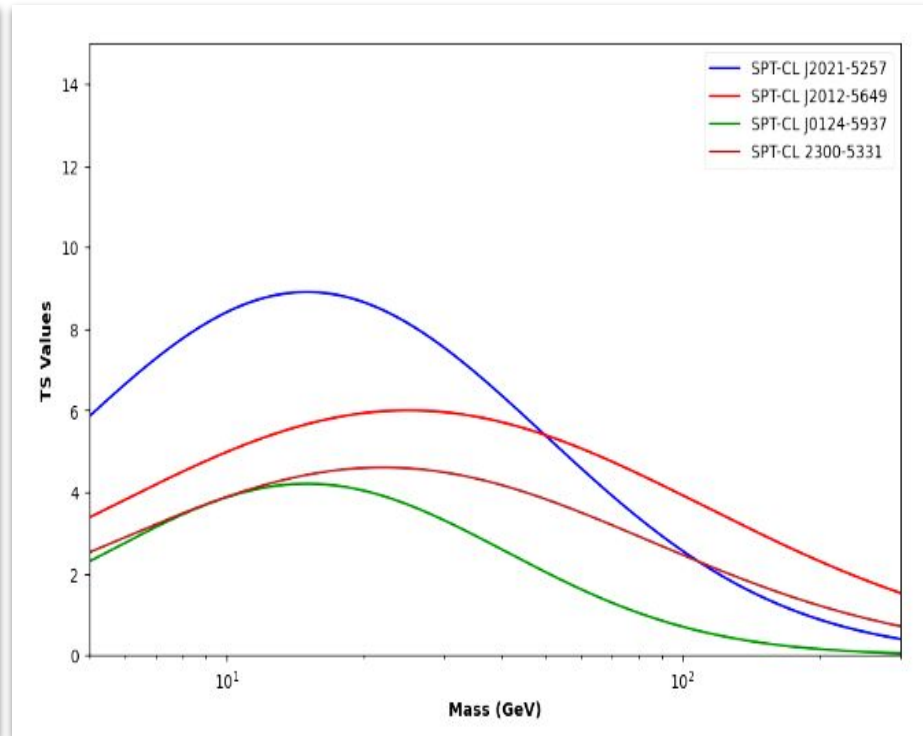


# Clusters with significance $> 2\sigma$

Clusters	TS Values
<b>SPT-CL J2021-5257</b>	<b>9.2</b>
SPT-CL J2012-5649	6.4
SPT-CL J2300-5331	4.8
SPT-CL J0124-5937	4.0



**TS as a function of the WIMP mass for clusters with  $TS \geq 4$  for the  $b\bar{b}$  annihilation channel.**



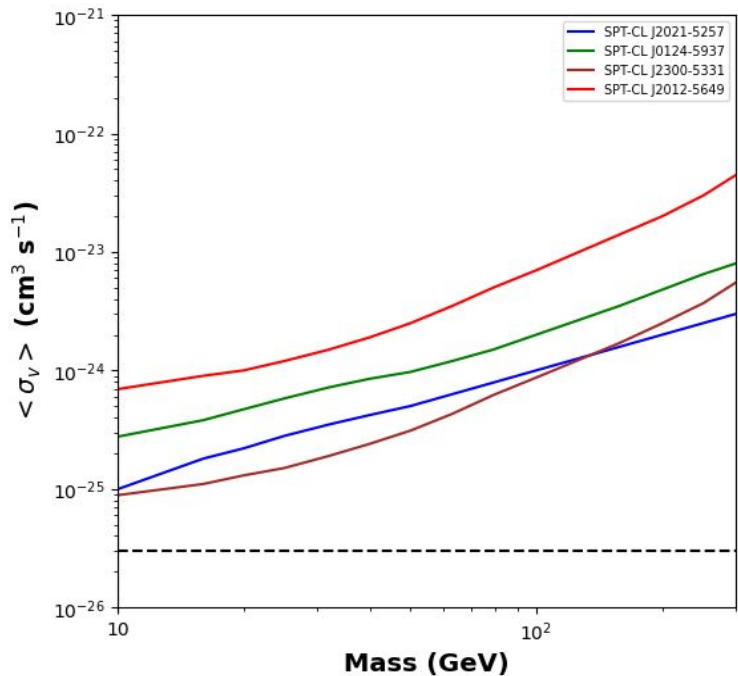
**TS as a function of WIMP mass for the  $\tau^+\tau^-$  annihilation channel.**

# Best-fit values for clusters with $TS > 4$

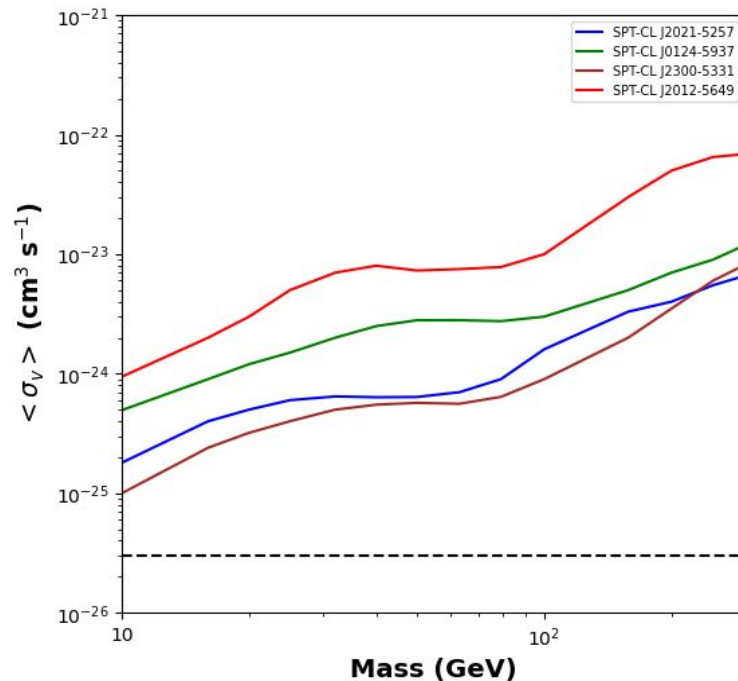
Clusters	Best-fit dark matter mass (GeV)	Best fit annihilation cross-section ( $\text{cm}^3 \text{s}^{-1}$ )
<b>SPT-CL J2021-5257</b>	<b><math>60.0 \pm 11.8</math></b>	<b><math>6.0 \pm 0.6 \times 10^{-25}</math></b>
SPT-CL J2012-5649	$90.0 \pm 4.5$	$5.9 \pm 0.5 \times 10^{-24}$
SPT-CL J2300-5331	$42.5 \pm 5.7$	$9.0 \pm 0.3 \times 10^{-25}$
SPT-CL J0124-5937	$65.0 \pm 3.8$	$3.5 \pm 0.2 \times 10^{-25}$

These values are in [conflict with the upper limits obtained from null searches for dark matter annihilation from Milky Way dwarf spheroidal galaxies](#), whose 95% c.l. limits on the velocity-averaged annihilation cross-section are around  $10^{-26} \text{ cm}^3 \text{ s}^{-1}$ . These enhanced TS values corresponding to  $(2-3)\sigma$  significance cannot be by-products of dark matter annihilation. They could be due to some astrophysical process resulting from cosmic interactions with gas and photons in the intracluster medium

# Upper Limits on annihilation cross-section



**95 % c.l. upper limits on the annihilation cross-section of WIMP dark matter for the  $b\bar{b}$  annihilation channel, considering the presence of substructures in the galaxy clusters with  $TS \geq 4$ .**

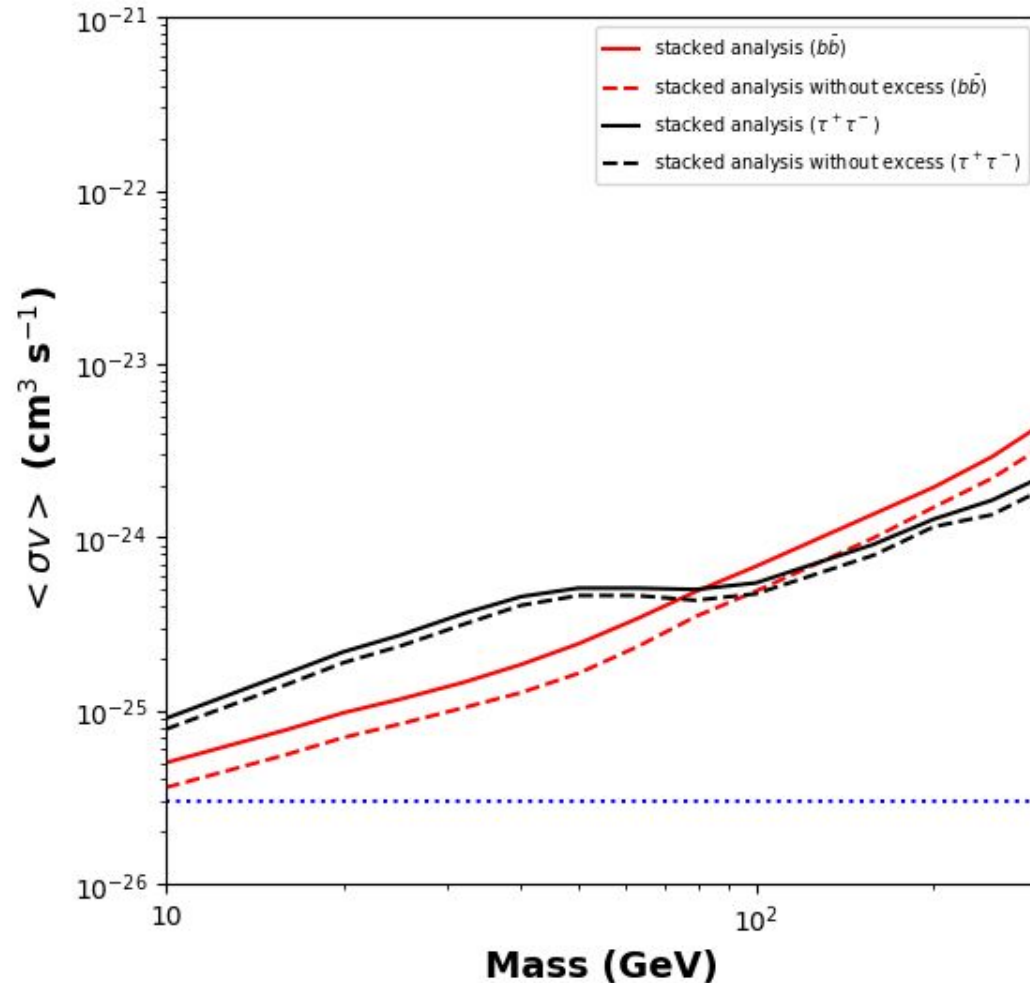


**95% c.l. upper limits for  $\tau^+\tau^-$  annihilation channel. The black solid line indicates the canonical thermal cross-section of  $3 \times 10^{-26} \text{ cm}^3 \text{ s}^{-1}$ .**

# Upper Limits on annihilation cross-section

- Amongst all 350 clusters, we found the most stringent limit for SPT-CL J0455-4159, viz.  $\langle\sigma v\rangle = 6.44 \times 10^{-26} \text{cm}^3 \text{s}^{-1}$  for  $m_\chi = 10 \text{ GeV}$  and  $b\bar{b}$  annihilation channel. The corresponding limit for  $\tau^+\tau^-$  annihilation channel for this cluster is given by  $\langle\sigma v\rangle = 8.26 \times 10^{-26} \text{cm}^3 \text{s}^{-1}$  for  $m_\chi = 10 \text{ GeV}$ .
- Among all the clusters with significance  $\geq 2\sigma$ , we found the most stringent limit for SPT-CL J2300-5331, viz.  $\langle\sigma v\rangle = 8.85 \times 10^{-26} \text{cm}^3 \text{s}^{-1}$  for  $m_\chi = 10 \text{ GeV}$  considering the  $b\bar{b}$  annihilation channel, and  $\langle\sigma v\rangle = 10.0 \times 10^{-26} \text{cm}^3 \text{s}^{-1}$  for  $m_\chi = 10 \text{ GeV}$  and considering the  $\tau^+\tau^-$  annihilation channel.

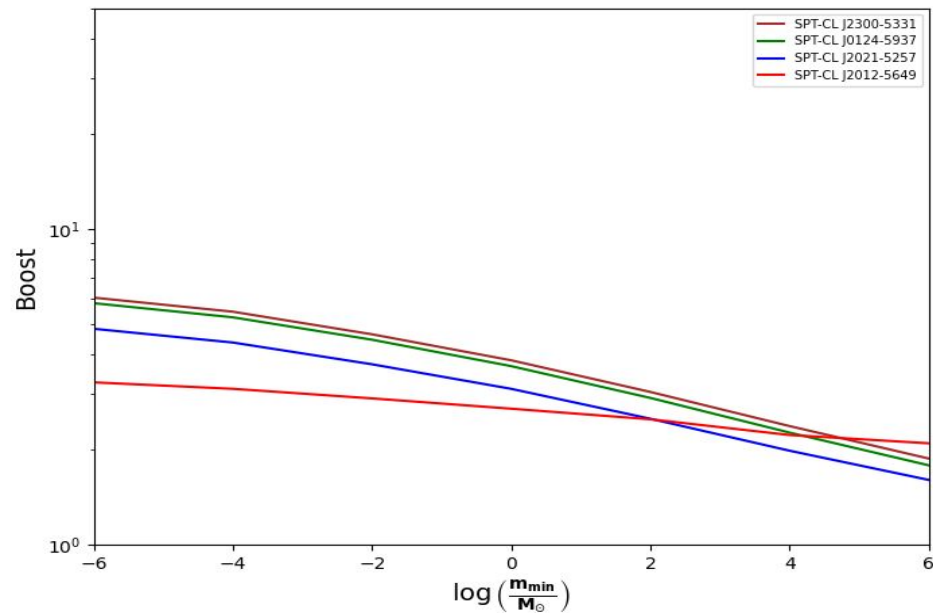
## STACKING RESULTS



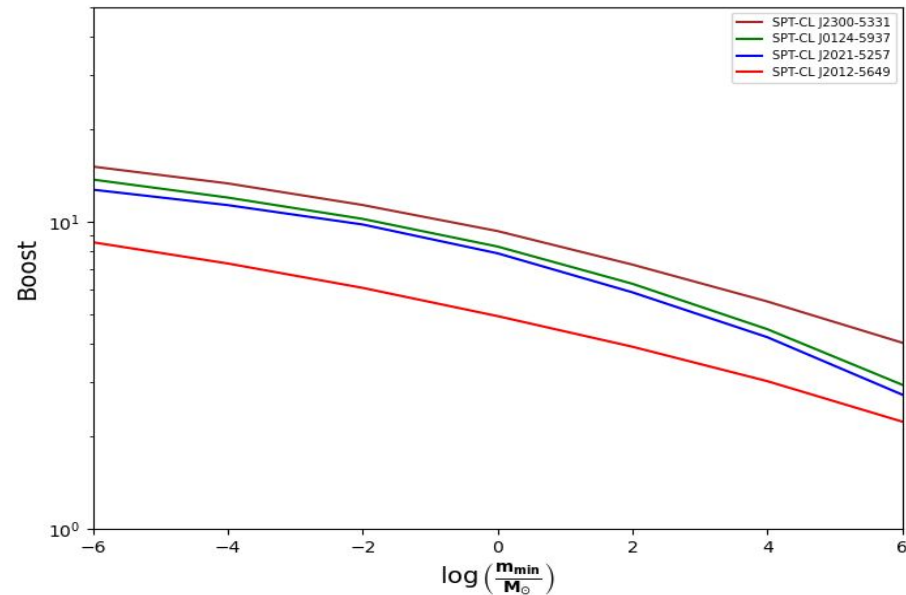
- 95% CL upper limits on the annihilation cross-section for the  $b\bar{b}$  (red) and  $\tau^+\tau^-$  (black) annihilation channels using the combined data from all clusters.
- The solid lines represent the results for all 350 clusters, while dashed lines show the limits when clusters with  $TS > 4$ . The dotted blue line shows the canonical thermal cross-section

# Boost Factor using different subhalo models

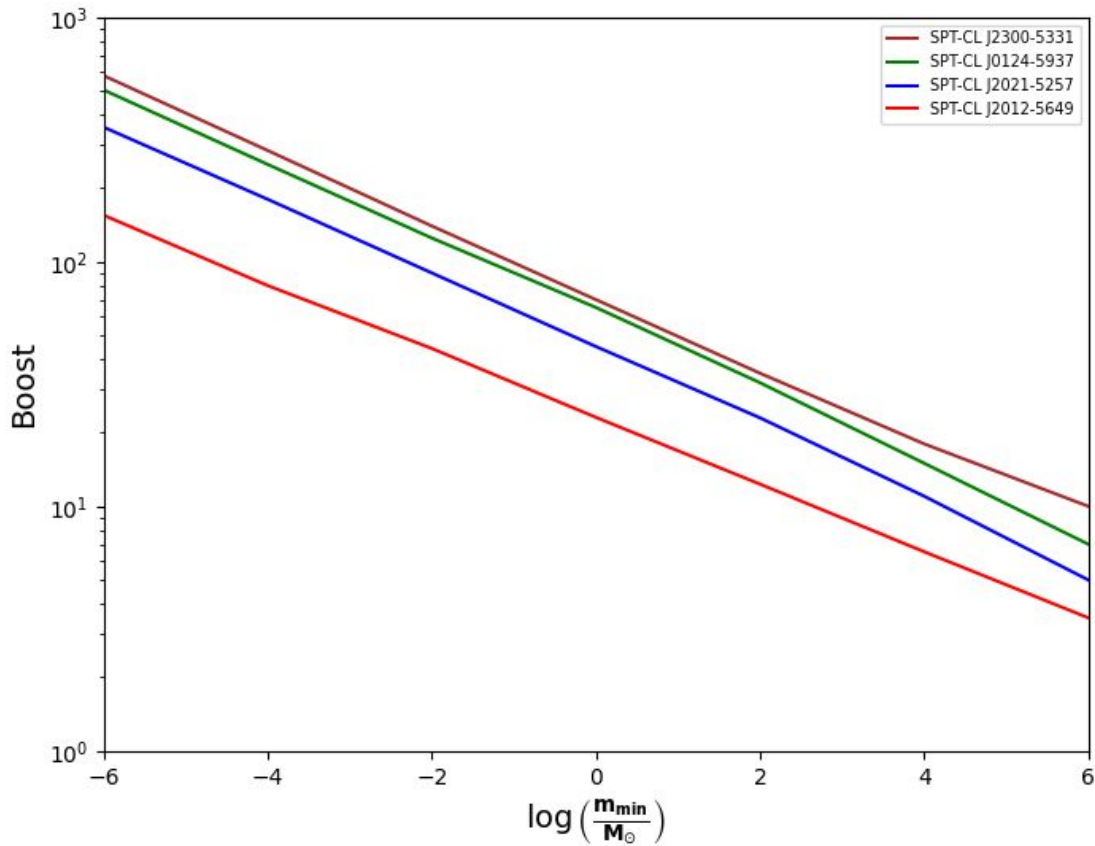
R. Bartels and S. Ando, Phys. Rev. D  
arXiv: 1507.08656



$$dN / dM = (0.03/M) (m/M)^{-1.9}$$



$$dN / dM = (0.012/M)(m/M)^{-2.0}$$



Phoenix  
Project

L. Gao, C. S. Frenk, A. Jenkins, V. Springel, and S.  
D. M. White, MNRAS. arXiv: 1107.1916



# Conclusion and Future Work

- In this work, we searched for gamma-ray emission between 1 and 300 GeV from dark matter annihilation in galaxy clusters. We analyzed 350 clusters selected from the SPT-SZ 2500 square degree survey, which provides a mass-limited sample.
- The analysis utilized 15.7 years of data from the Fermi-LAT telescope and employed the DMFIT template. Notably, we identified a  $3\sigma$  emission signal from the galaxy cluster SPT-CL J2021-5257.
- Although prima-facie, we found  $3\sigma$  detection evidence from SPT-CL J2021-5257, the estimated annihilation cross-section is in conflict with upper limits from Milky way dwarf spheroidal galaxies. Therefore, we conclude that the enhanced signal seen for SPT-CL J2021-5257 cannot be due to dark matter annihilation.
- We obtained a marginal significance of around  $2\sigma$  for three other clusters: SPT-CL J2012-5649, SPT-CL J0124-5937 and SPT-CL J2300-5331. All the remaining clusters showed null results and the TS values were consistent with background.
- Moving forward, we plan to expand this analysis to encompass all galaxy clusters detected in ongoing X-ray and SZ surveys such as eROSITA and SPTPol.



THANK YOU ! OPEN FOR QUESTIONS

# BACKUP SLIDES

- The best fit WIMP mass for SPT-CL J2021-5257 is found to be  $64.0 \pm 11.8$  GeV, whereas the best-fit value of  $\langle\sigma v\rangle = 6.0 \pm 0.6 \times 10^{-25} \text{cm}^3 \text{s}^{-1}$  for this cluster assuming a  $b\bar{b}$  annihilation channel.
- For SPT-CL J2012-5649, SPT-CLJ 0124-5937, and SPT-CL J2300-5331, the best-fit masses were found to be  $91.0 \pm 4.5$  GeV,  $42.5 \pm 5.7$  GeV, and  $65.0 \pm 3.8$  GeV, respectively. The corresponding best-fit values of  $\langle\sigma v\rangle$  for the  $b\bar{b}$  channel were  $5.9 \pm 0.5 \times 10^{-24} \text{cm}^3 \text{s}^{-1}$ ,  $9.0 \pm 0.3 \times 10^{-25} \text{cm}^3 \text{s}^{-1}$  and  $3.5 \pm 0.2 \times 10^{-25} \text{cm}^3 \text{s}^{-1}$ , respectively.
- The best-fit dark matter mass for SPT-CL J2021-5257 for the  $\tau^+ \tau^-$  annihilation channel is found to be  $15.3 \pm 4.1$  GeV, whereas the best-fit annihilation cross-section is given by  $\langle\sigma v\rangle = 3.5 \pm 0.9 \times 10^{-25} \text{cm}^3 \text{s}^{-1}$ .
- Similarly, for SPT-CL J2012-5649, SPT-CLJ0124-5937, and SPT-CL J2300-5331 we found the best-fit mass as  $24.0 \pm 1.5$ ,  $15.0 \pm 2.8$ , and  $22.0 \pm 2.1$  GeV, respectively, whereas the best-fit values of  $\langle\sigma v\rangle$  are equal to  $5.0 \pm 0.4 \times 10^{-24} \text{cm}^3 \text{s}^{-1}$ ,  $6.3 \pm 0.8 \times 10^{-25} \text{cm}^3 \text{s}^{-1}$  and  $2.8 \pm 0.4 \times 10^{-25} \text{cm}^3 \text{s}^{-1}$ , respectively for  $\tau^+ \tau^-$  annihilation channel.
- These values are in conflict with the upper limits obtained from null searches for dark matter annihilation from Milky Way dwarf spheroidal galaxies, whose 95% c.l. limits on the velocity-averaged annihilation cross-section are around  $10^{-26} \text{cm}^3/\text{sec}$ . The significance we found is less than  $5\sigma$ .

# Conclusion and Future Work (Contd...)

- We note among the clusters with  $\geq 2\sigma$  significance is **SPT-CL J2012-5649 (TS = 6.2)**, which is **spatially coincident with the merging cluster Abell 3667**. We note that this cluster was **detected with the highest significance ( $> 6\sigma$ ) in our previous work on gamma-ray searches using a point source template**.
- Moving forward, we plan to expand this analysis to encompass all galaxy clusters detected in ongoing **X-ray and SZ surveys such as eROSITA and SPTPol**.
- This work is submitted to JCAP and can be found at arXiv paper: [arXiv 2407.10189](https://arxiv.org/abs/2407.10189)

Thank You and I am open to  
Questions

# Analysis Process (Contd...)

- For the **spectral analysis**, we utilized the **comobsmodel** tool to fit source emission models to the COMPTEL data.
- We then employed the **comlifit** tool to perform **maximum likelihood fitting** of the COMPTEL data utilizing the iterative **SRCLIX(Source Likelihood) algorithm**.
- Furthermore, the **instrumental background Model** was modelled using the **BGDLIXE(Background Likelihood)** background computation model. It enables a more accurate and reliable characterization of the true MeV gamma-ray signal originating from the target galaxy clusters.
- We leveraged the **comlixmap** tool to construct **Test Statistics** by applying the **SRCLIX** on every test source position.
- We also constructed the **Spectral Energy Distribution (SED)** plots using the **csspec** tool and **obtained upper limits (in case of null results)** with the **ctulimit** tool.
- These SED plots, constructed within the energy range of 0.75-30 MeV using **16 logarithmic energy bins** and the **BINS spectrum** generation method, visually **represent the upper limits on the flux density** of potential gamma-ray sources within the clusters

# RESULTS

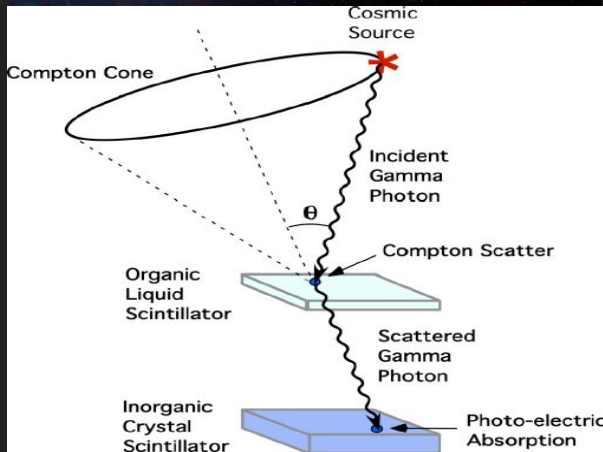
- We conducted the analysis for the clusters in our sample using  $b\bar{b}$  and  $\tau^+\tau^-$  annihilation channels for all 350 clusters and calculated their J-Factors and TS values.
- Among all the clusters, SPT-CL J2021-5257 shows the maximum TS value of 9, corresponding to  $3\sigma$  emission using the dark matter template for energy range 1-300 GeV. We also performed the analysis for SPT-CL J2021-5257 by extending the lower energy range to 100 MeV and found that TS value decreases to 7, corresponding to  $2.6\sigma$  significance.
- Other clusters, such as SPT-CL J2012-5649, SPT-CL J0124-5937, and SPT-CL J2300-5331 show TS values corresponding to  $\sim 2 - 2.5\sigma$  significance, suggesting a weaker detection significance.

# Search for soft gamma-rays from clusters



NASA

- Compton Gamma Ray Observatory was launched on **April 5, 1991**. It had four instruments which covered the high energy electromagnetic spectrum from **30 keV to 30 GeV**: **BATSE, OSSE, COMPTEL, and EGRET**. It operated from **1991-2000**.



COMPTEL  
working  
process

- The Imaging Compton Telescope (**COMPTEL**) used **two layers of gamma ray detectors** to study gamma rays ranging from **0.75 to 30 MeV**. **COMPTEL is the only instrument which is sensitive in this energy range.**
- At lower energies around 1 MeV, Point Spread Function (PSF) of COMPTEL is around  $4.4^\circ$  whereas it improves significantly to  $1.7^\circ$  at 30 MeV.

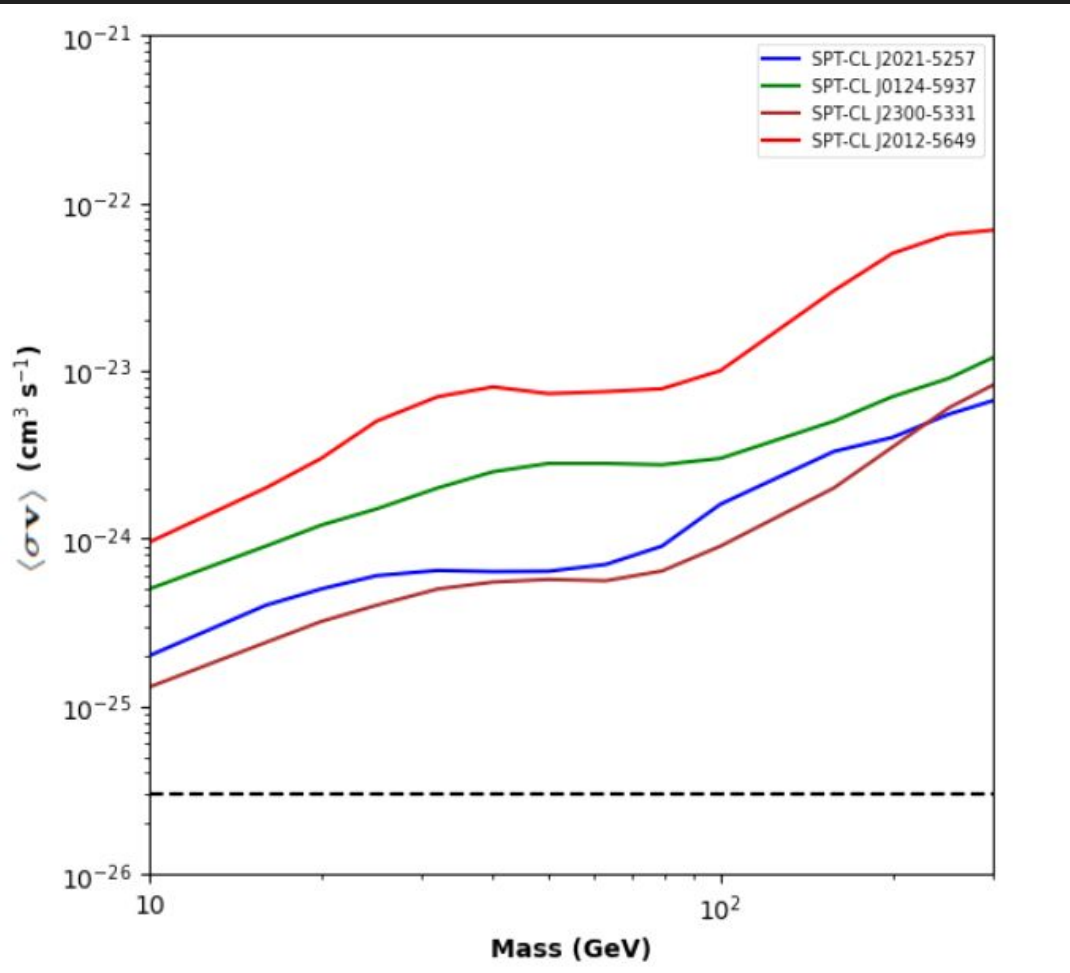


# Analysis Process

- We carried out a systematic search within a  $10^\circ$  radius surrounding each target cluster utilizing the **ctools** software package.
- We employed the **comobsselect** tool to **extract the viewing periods** for the clusters, applying **precise filtering** based on their coordinates and a specified radius. The selection process effectively **removes unwanted background noise**.
- Using the **comobsbin** tool, we implemented **energy binning to optimize the signal-to-noise ratio**. We used **16 logarithmically-spaced energy bins** spanning the **0.75-30 MeV** range.
- For **SPT-CL J2012-5649, El Gordo, VIRGO and Bullet Cluster**, we combined the data from **two or more distinct viewing periods** using the **comobsadd** tool with **80 bins each in the  $\chi$  and  $\psi$  directions**, where  $\chi$  and  $\psi$  are the Compton scattering directions. Unlike the other clusters, for **Coma cluster**, we got data from only **one viewing period**.
- Our search analysis was done using three different templates, viz. **point source, radial disk and radial Gaussian templates**

# Search for soft gamma-rays from clusters

- The telescope field of view was about **one steradian**. It was sensitive to gamma-rays between **0.75- 30 MeV**, where the energy and angular resolution ranged between **5-8% and (1.7 – 4.4)°**, respectively depending on the photon energy.
- During its 9.7 years of operation, COMPTEL did about **340 distinct pointings** (with a duration of **two weeks**), where each pointing had a field of view **radius of around 30°**
- A large number of astrophysical sources have been detected by COMPTEL such as pulsars, AGNs, X-ray binaries, gamma-ray bursts, solar flares, 26Al, supernova remnants, extragalactic diffuse gamma-ray background, etc
- The **targets we consider for our analysis include VIRGO, Coma, SPT-CL J2012-5649, Bullet (SPT-CL J0658-5556), and El Gordo (SPT-CL J0102-4915) clusters.**



Similar to last figure but here we show the 95% c.l. upper limits for  $\tau^+\tau^-$  annihilation channel

# SOURCE MODEL DEFINITIONS FOR GTLIKE

- ★ Two types of sources can be defined, **Point Source and Diffuse Source**. Each type of source model is comprised of a spectral and a spatial model component.
- ★ The available point source spectral models are: PowerLaw, BrokenPowerLaw, PowerLaw2, LogParabola, ExpCutoff, ConstantValue, Gaussian etc. The **preferred spectral model is Power law, whose XML model definition and function form is shown in the right.**
- ★ **Power-law index or spectral index** governs the shape of the **power-law distribution**. It determines how quickly the intensity of gamma rays decreases with increasing angle from the source.
- ★ The **prefactor** sets the overall scale of the emission, representing the **intensity of the source at the reference Energy. It is essentially a normalization constant.**

## PowerLaw:

Example: [XML Model Definition](#)

This function has the form:

$$\frac{dN}{dE} = N_0 \left( \frac{E}{E_0} \right)^\gamma$$

where the parameters in the XML definition have the following mappings:

- Prefactor =  $N_0$
- Index =  $\gamma$
- Scale =  $E_0$

# LAT DATA PRODUCTS: EVENT RECONSTRUCTION & BACKGROUND MODELS

- ★ The LAT performance is governed primarily by three things: **LAT hardware design, Event reconstruction algorithms and Background selections and event quality selections.**
- ★ **Pass 8 is the latest data release.** It includes **updated calibration, background models, and event reconstruction techniques.** Pass 8 data is often **recommended** for new analyses.
- ★ In Pass 8: the **ULTRACLEANVETO class at all energies** or the **SOURCEVETO** class above a couple of GeV are ideal for analysis of large regions that are more sensitive to spectral features caused by instrumental backgrounds.
- ★ LAT data requires **Background models of Galactic diffuse and isotropic emission for analysis.** The preferred version of the Interstellar Emission Model for the analysis of Pass 8 data is **gll\_iem\_v07.fits.**

Standard Hierarchy for LAT Event Classes				
Event Class	evclass	Photon File	Extended File	Description
P8R3_TRANSIENT020	16		X	Transient event class with background rate equal to two times the A10 IGRB reference spectrum.
P8R3_TRANSIENT010	64		X	Transient event class with background rate equal to one times the A10 IGRB reference spectrum.
P8R3_SOURCE	128	X	X	This event class has a residual background rate that is comparable to P7REP_SOURCE. This is the recommended class for most analyses and provides good sensitivity for analysis of point sources and moderately extended sources.
P8R3_CLEAN	256	X	X	This class is identical to SOURCE below 3 GeV. Above 3 GeV it has a 1.3-2 times lower background rate than SOURCE and is slightly more sensitive to hard spectrum sources at high galactic latitudes.
P8R3_ULTRACLEAN	512	X	X	This class has a background rate very similar to ULTRACLEANVETO.
P8R3_ULTRACLEANVETO	1024	X	X	This is the cleanest Pass 8 event class. Its background rate is 15-20% lower than the background rate of SOURCE class below 10 GeV, and 50% lower at 200 GeV. This class is recommended to check for CR-induced systematics as well as for studies of diffuse emission that require low levels of CR contamination.

- ★ Using the **scale** attribute is necessary to ensure that the parameters describing the objective function, **-log(likelihood)** have values lying roughly within an order-of-magnitude of each other. The **free** attribute determines whether the parameter will be allowed to be fixed or free in the fitting process.
- ★ In most analysis, ours including **spectral index is fixed to -2 whereas Prefactor is allowed to vary.**
- ★ Four spatial models are available for analysis: SkyDirFunction, ConstantValue, SpatialMap and MapCubeFunction.
- ★ We can perform extended source analysis using SkyDirFunction. **The Radial Models available are RadialGaussian and RadialDisk.**

#### RadialDisk

```
<spatialModel type="RadialDisk">  
<parameter free="0" max="10" min="0" name="Radius" scale="1" value="0.2" />  
<parameter free="0" max="360" min="-360" name="RA" scale="1" value="166.1138" />  
<parameter free="0" max="90" min="-90" name="DEC" scale="1" value="38.2088" />  
</spatialModel>
```

#### RadialGaussian

```
<spatialModel type="RadialGaussian">  
<parameter free="0" max="10" min="0" name="Sigma" scale="1" value="0.2" />  
<parameter free="0" max="360" min="-360" name="RA" scale="1" value="166.1138" />  
<parameter free="0" max="90" min="-90" name="DEC" scale="1" value="38.2088" />  
</spatialModel>
```

# DMFIT Template

## DMFitFunction

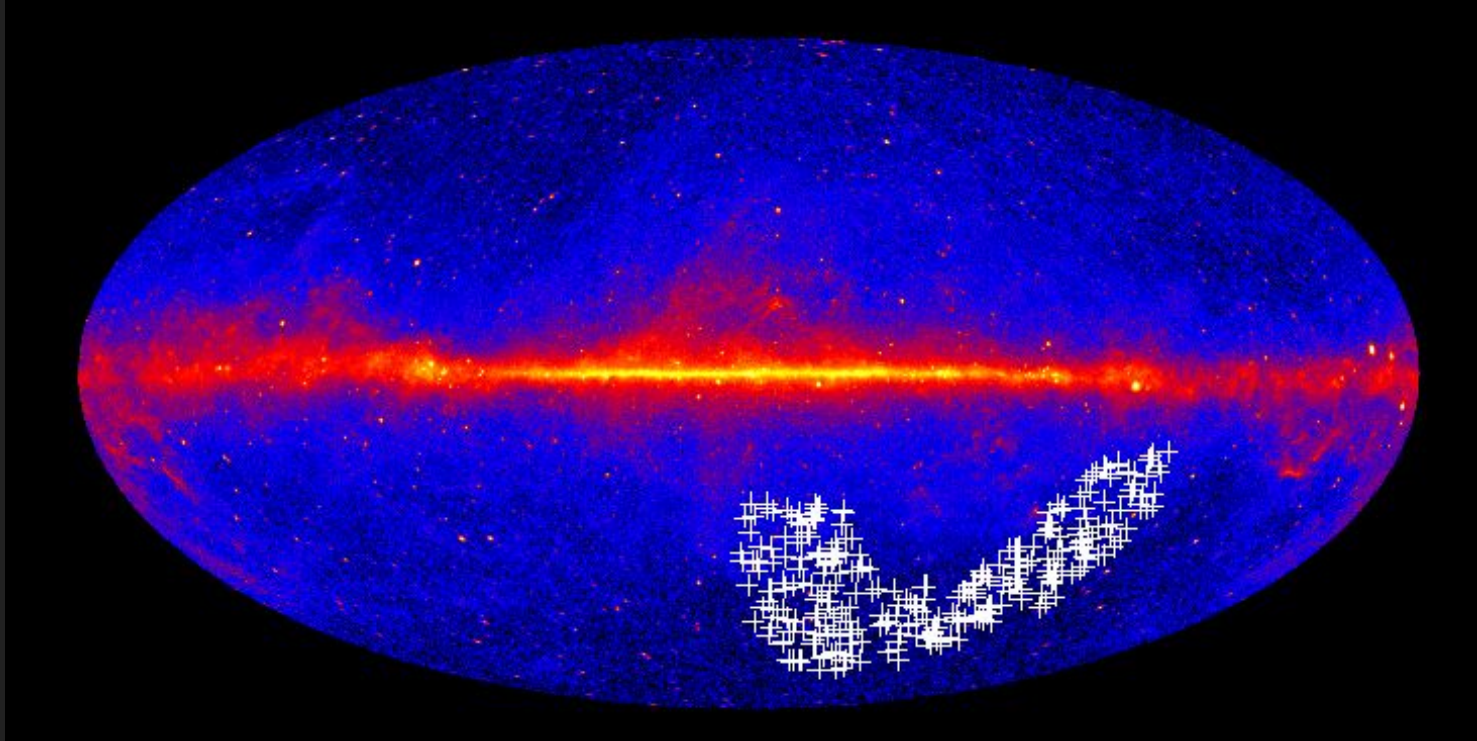
```
<source name="DM_Example" type="PointSource">
<spectrum file="$(BASE_DIR)/data/Likelihood/gammamc_dif.dat" type="DMFitFunction">
<parameter error="1." free="0" max="1.e+5" min="1.e-5" name="norm" scale="1.e+20" value="5.0"
/>
<parameter error="1." free="0" max="5000.0" min="0." name="sigmav" scale="1.e-26" value="3.0"
/>
<parameter error="1." free="0" max="5000.0" min="1." name="mass" scale="1.0" value="10"/>
<parameter error="0.1" free="0" max="1.0" min="0.0" name="bratio" scale="1.0" value="1"/>
<parameter free="0" max="10" min="1" name="channel0" scale="1.0" value="4"/>
<parameter free="0" max="10" min="1" name="channel1" scale="1.0" value="1"/>
</spectrum>
<spatialModel type="SkyDirFunction">
<parameter free="0" max="360" min="-360" name="RA" scale="1.0" value="128.8272"/>
<parameter free="0" max="90" min="-90" name="DEC" scale="1.0" value="-45.1762"/>
</spatialModel>
</source>
```

# INSTRUMENT RESPONSE FUNCTIONS (IRFS) & POINT SPREAD FUNCTION (PSF)

- ★ To evaluate the LAT response, a dedicated **Monte Carlo** simulation is performed. A large number of gamma-ray events are simulated in order to cover all **possible photon inclination angles** and **energies** with good statistics. This is based on the best available representation of the physics interactions, the instrument, and the on-board and ground processing to produce event classes (**Atwood et al. 2009 and Ackerman et al. 2012**). The comparison between the properties of the simulated events within a given event class and the input photons gives the **Instrument Response Functions (IRFs)**.
- ★ Each event class and event type selection has its own IRFs. Pass 8 data release defines **three event type partitions: FRONT/BACK (two types), PSF (four types), and EDISP (four types)**. In the typical usage scenario in which all events within a class are selected (equivalent to **evtype=3**) the Fermi Tools will apply the response function for the sum of **FRONT and BACK events**.
- ★ **Point spread function** for the LAT is a function of an incident photon's energy and inclination angle, and the event class.



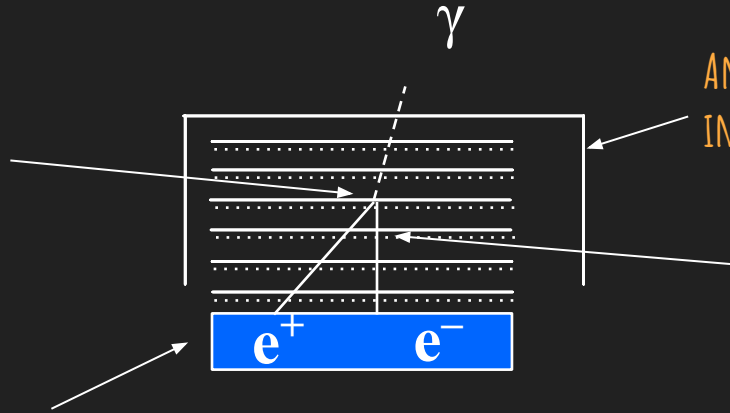
# ANALYSIS AND RESULTS



The Fermi-LAT count map in galactic coordinates based on the 4FGL-DR4 catalog, using 12 years of survey data . The white colored plus sign depicts the locations of the 300 SPT-SZ galaxy clusters we used in our analysis. The bright, diffuse glow running along the middle of the map, shows the central plane of our Milky Way.

# PAIR CONVERSION TELESCOPE – BASIC PICTURE

GAMMA RAY CONVERTS TO AN  $e^+ e^-$  PAIR IN A HIGH DENSITY FOIL LAYER.

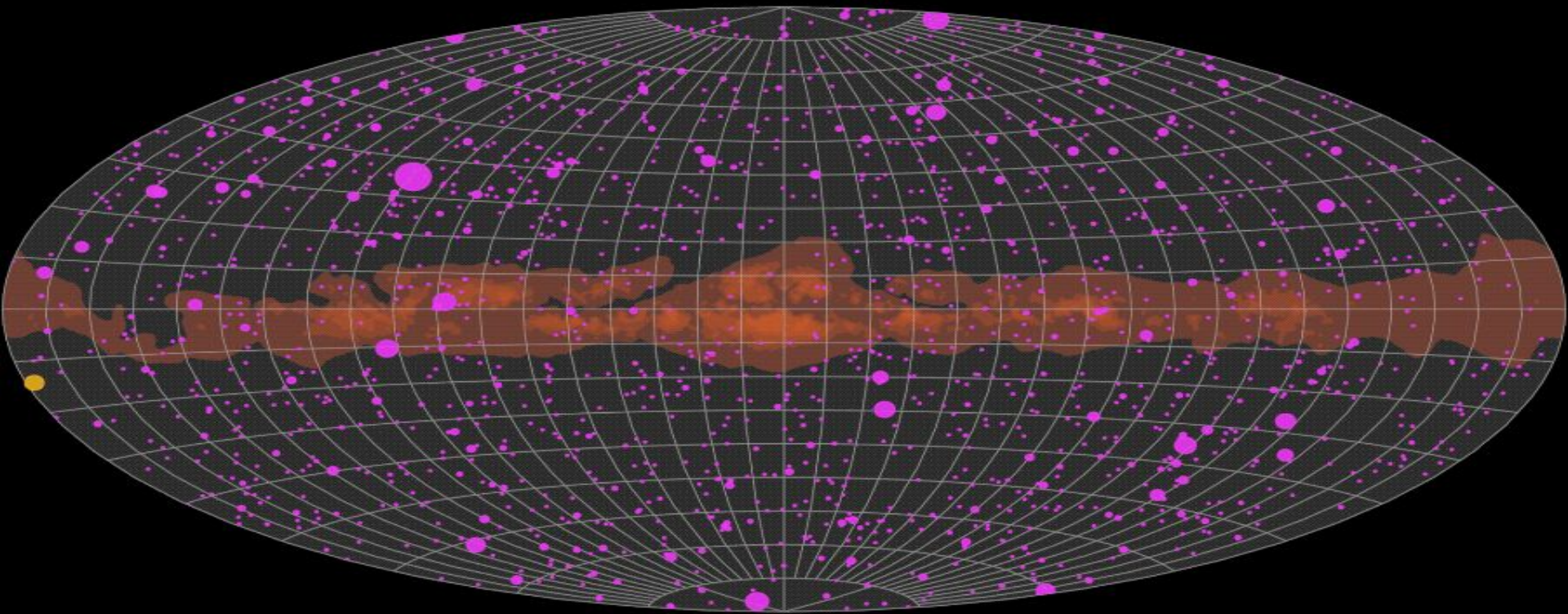


AN ANTI-COINCIDENCE SHIELD DETECTS AND VETOS INCOMING CHARGED PARTICLES.

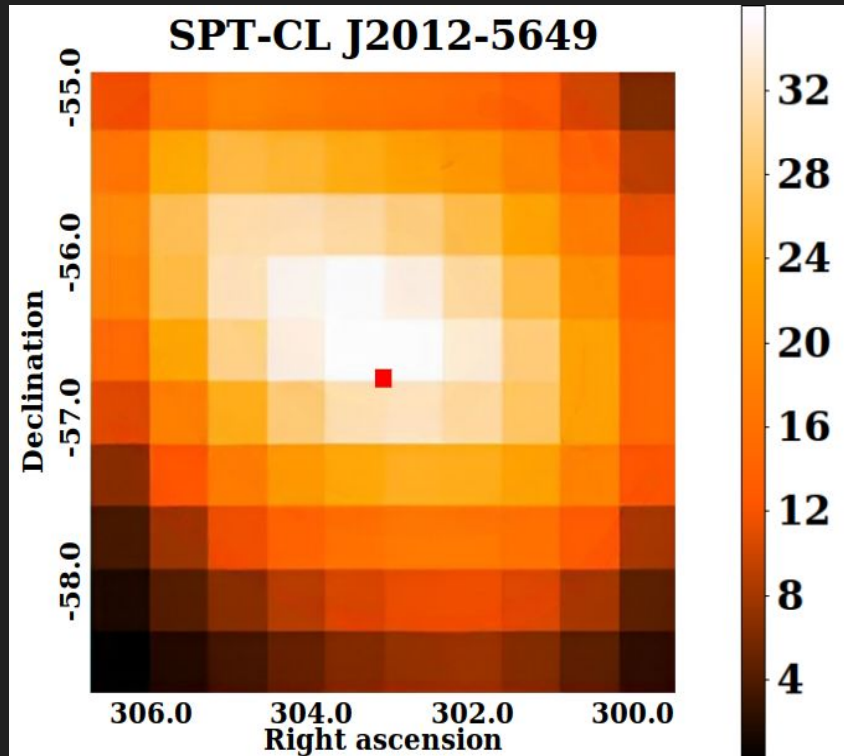
THE TRACKS OF CHARGED PARTICLES IN THE INSTRUMENT ARE RECORDED BY SENSORS.

THE PHOTON ENERGY IS DETERMINED FROM MEASURED ENERGY DEPOSITED IN THE CALORIMETER.

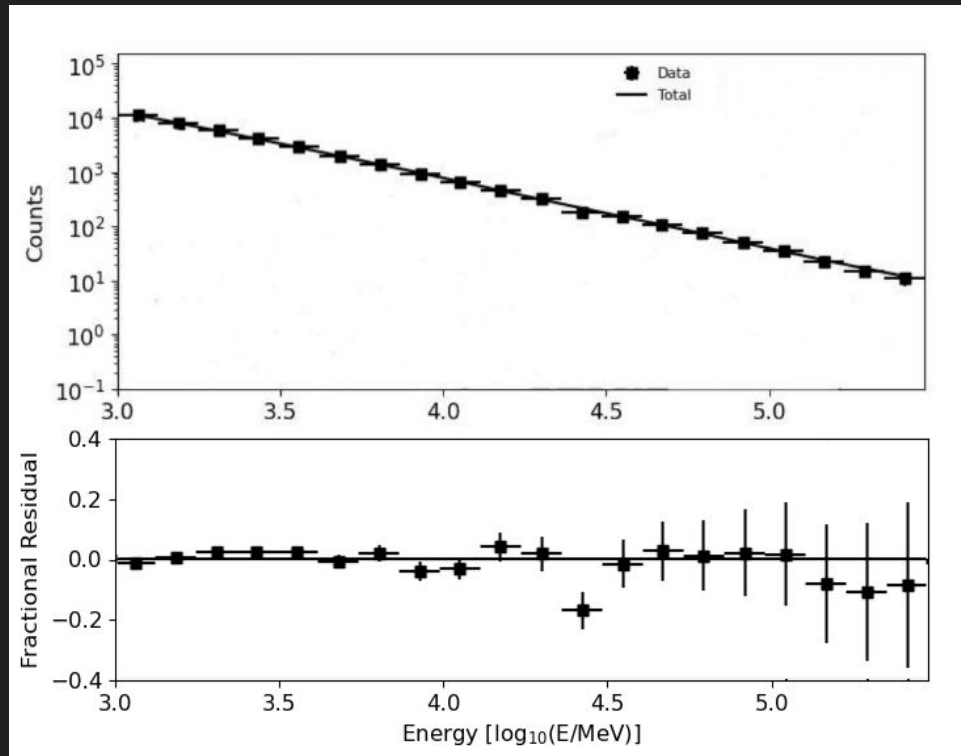
THE TRACKS ARE USED TO DETERMINE THE DIRECTION OF THE GAMMA-RAY SOURCE.



COSMIC GAMMA-RAY FIREWORKS SHOW IN THIS ANIMATION USING JUST A YEAR OF DATA FROM THE LARGE AREA TELESCOPE (LAT) ABOARD NASA'S FERMI GAMMA-RAY SPACE TELESCOPE. EACH OBJECT'S MAGENTA CIRCLE GROWS AS IT BRIGHTENS AND SHRINKS AS IT DIMS. THE YELLOW CIRCLE REPRESENTS THE SUN FOLLOWING ITS APPARENT ANNUAL PATH ACROSS THE SKY



**TS map for SPT-CL J2012-5649 (Abell 3667) with significance  $> 5\sigma$**



**Top: Observed photons in energy bins from 1-300 GeV and the cumulative model of the total emission all the 4FGL-DR4 source diffuse emission templates and the observed signal from SPT-CL J2012-5649. Bottom: The fractional residuals given by (counts-model)/model, determined within 5° for SPT-CL J2012-5649.**

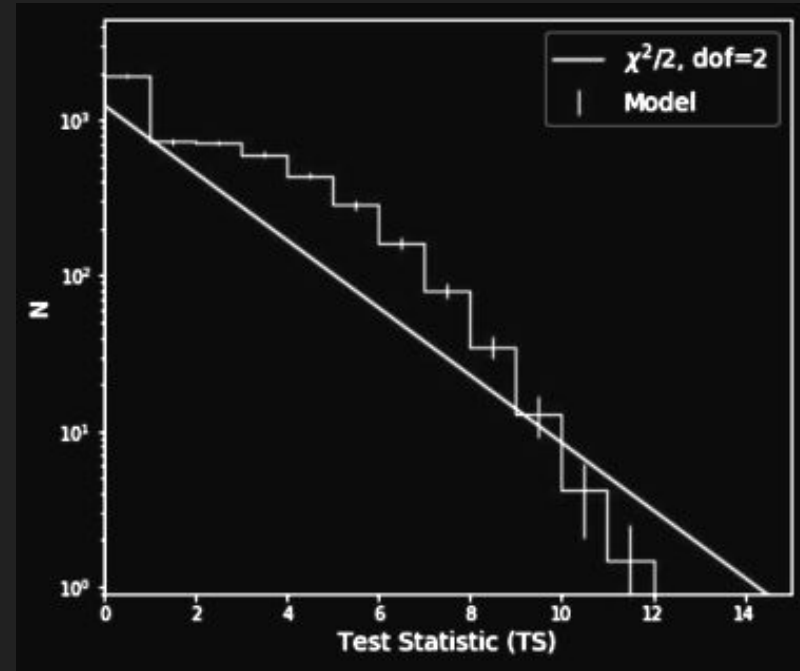
# Test statistics

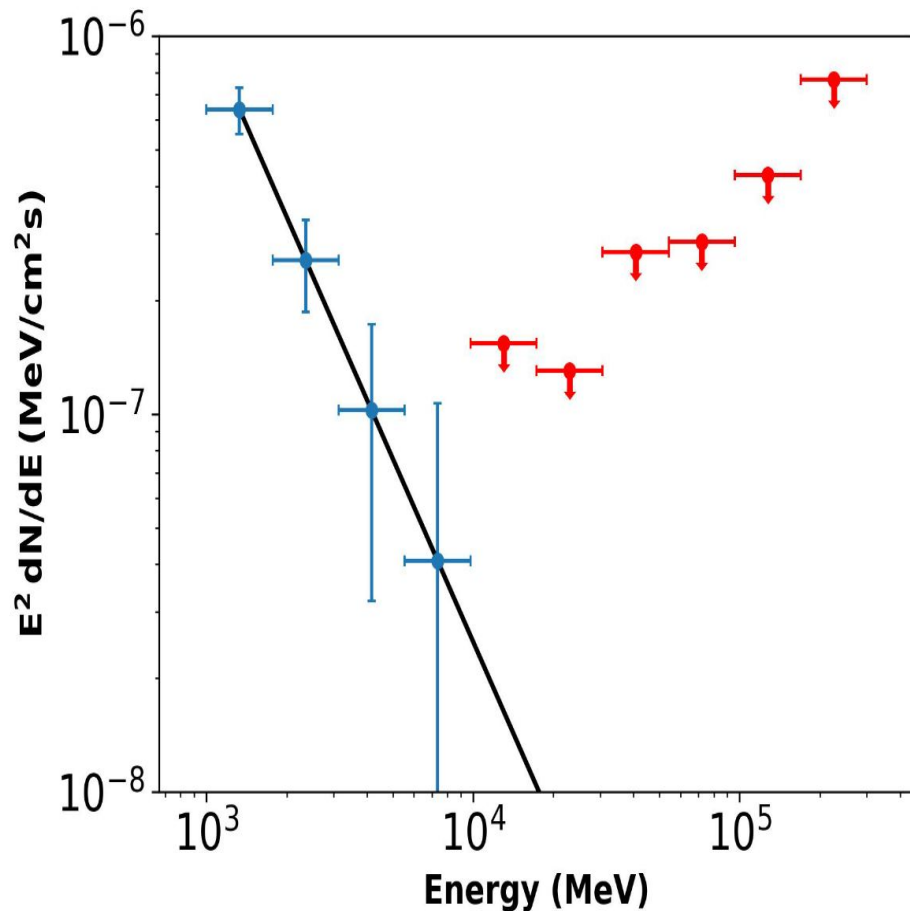
$$TS = 2 \times (\ln L - \ln L_0)$$

- ★ **TS value reflects the significance of the source.** Here,  $L$  is the Likelihood of source being present (alternate hypothesis) and  $L_0$  is the Likelihood of no source being present (null hypothesis).

$$\sigma = \sqrt{TS}$$

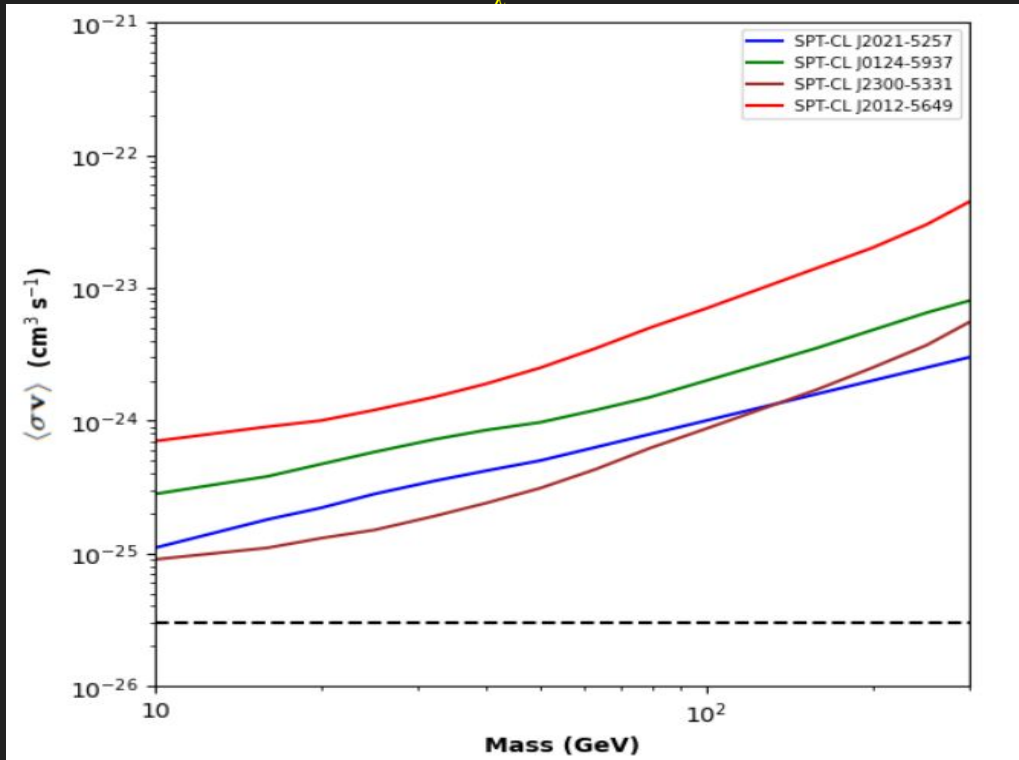
- ★ In the limit of a large number of counts, Wilks (1938) Theorem states that the **TS for the null hypothesis is asymptotically distributed as  $\chi^2$  distribution.**
- ★ TS of noise follows  $\chi^2 / 2$  distribution.
- ★ **Larger TS** indicates that the null hypothesis is incorrect (i.e., a **source really is present**), which can be quantified.





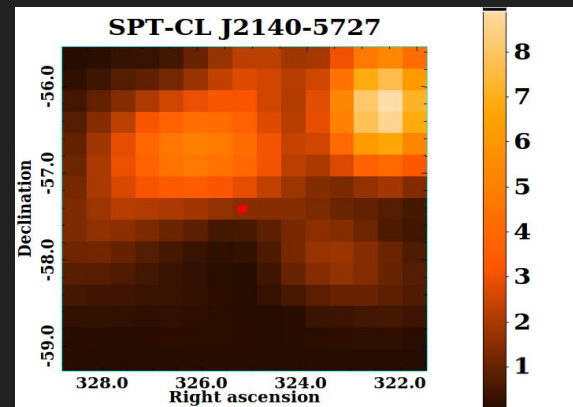
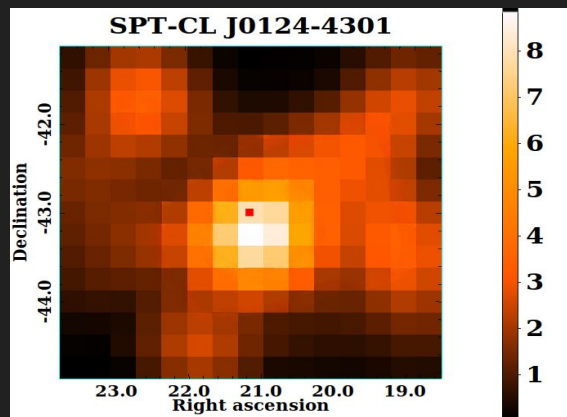
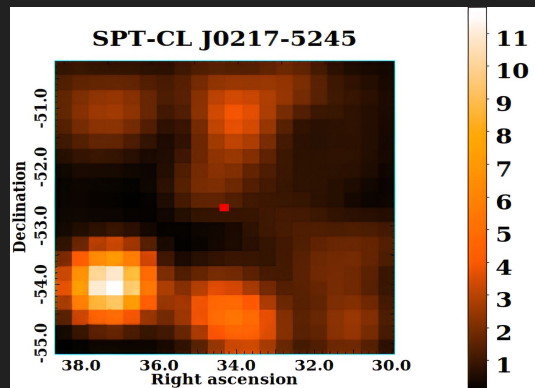
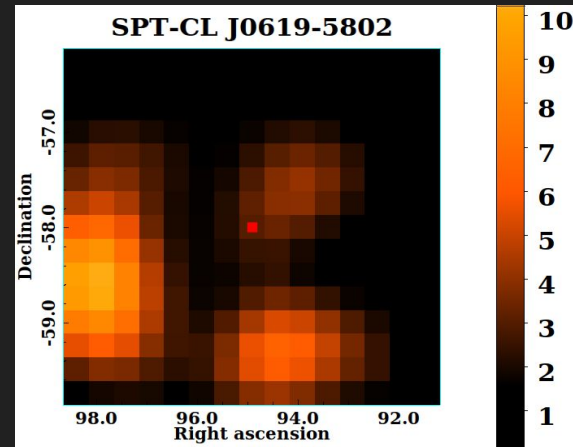
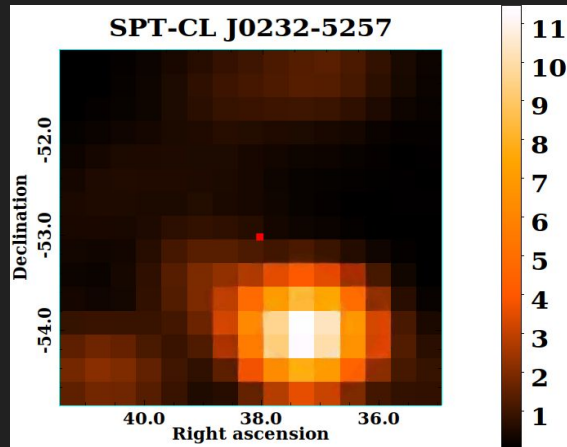
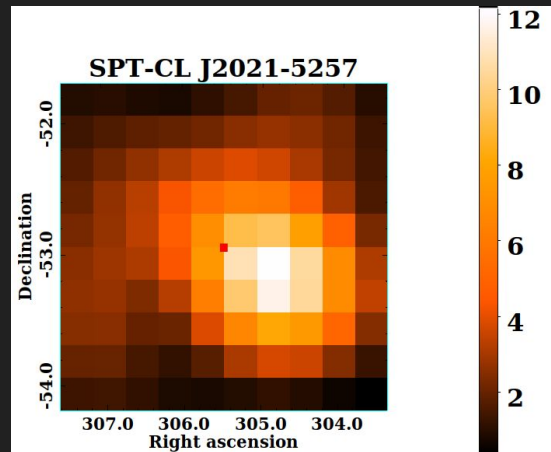
- ★ The differential energy spectrum from SPT-CL J2012-5649 obtained using easyFermi.
- ★ The solid line shows the power-law fit with the best-fit spectral index given by  $\gamma = -3.61 \pm 0.329$ .
- ★ The blue data points show the measured differential energy spectrum, while the red point represent upper limits. All the signal is observed at energies  $\leq 10$  GeV, and beyond that we obtain upper limits

- We calculate **upper limits** for the dark matter annihilation cross-section for these cluster. Our upper limits are mostly in agreement with other works, which have obtained limits on annihilation cross-section. Among all the clusters with **significance  $\geq 2\sigma$** , we found the **most stringent limit for SPT-CL J2300-5331**, viz.  $\langle\sigma v\rangle = 9 \times 10^{-26} \text{cm}^3 \text{s}^{-1}$  for  $m_\chi = 10 \text{ GeV}$  and  $b\bar{b}$  annihilation channel and  $\langle\sigma v\rangle = 10.3 \times 10^{-26} \text{cm}^3 \text{s}^{-1}$  for  $m_\chi = 10$



**95 % c.l. upper limits** on the annihilation cross-section of WIMP dark matter for the  $b\bar{b}$  annihilation channel, **considering the presence of substructures in the galaxy clusters with  $TS \geq 4$** . The black solid line indicates the canonical thermal cross-section of  $3 \times 10^{-26} \text{cm}^3 \text{s}^{-1}$

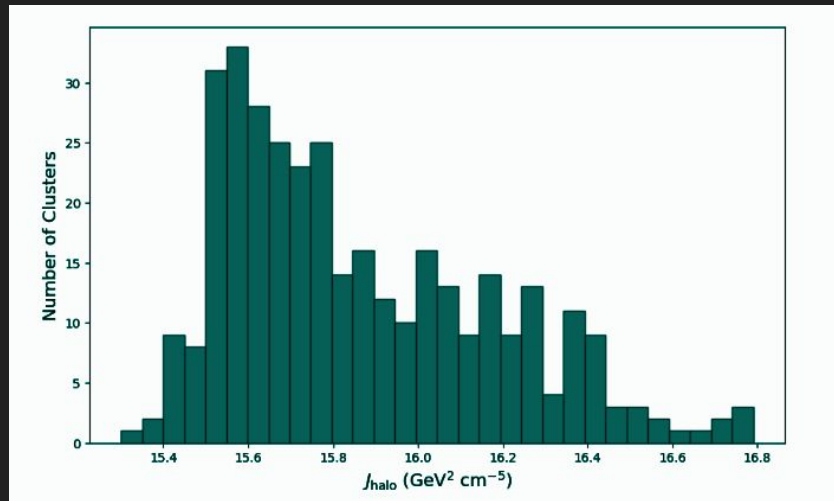
# TS MAPS OF GALAXY CLUSTERS $3\sigma < \text{SIGNIFICANCE} < 5\sigma$





# CONCLUSIONS AND FUTURE WORK

- ★ We searched for gamma-ray emission with energies between **1-300 GeV** from galaxy clusters, selected from the **SPT-SZ 2500 sq. degree survey**.
- ★ We used **15 years of Fermi-LAT data** and **point-source templates** for these searches. This analysis was done using **300 SPT-SZ galaxy clusters**, after sorting them in **descending order based on their  $M_{500}/z^2$  values**.
- ★ Among these clusters, we found statistically significant emission from **SPT-CL J2012-5649 (Abell 3667)** with a detection significance of  **$6.1\sigma$** . The detection significance reduces to about  **$2.5\sigma$**  if we use **non-point source templates or search in a higher energy range from 10 to 300 GeV**.
- ★ We also plotted the **SED graph**. The **signal is observed upto 10 GeV**, while the **spectral index is equal to  $-3.61 \pm 0.33$** . Above 10 GeV, we only obtain upper limits, which is consistent with the results from the MLE analysis in this energy range.
- ★ We note that there are **six radio galaxies from the SUMSS catalogue within  $0.2^\circ$  of this cluster**, which is within the Fermi-LAT PSF at this energy. Therefore, we cannot definitely conclude that the gamma-ray emission detected for SPT-CL J2012-5649 is coming from the ICM as opposed to radio sources contributing to this emission.
- ★ We also found **six other clusters with significance between  $3-5\sigma$** .
- ★ **Manuscript based on the above work has been published in JCAP DOI: 10.1088/1475-7516/2024/01/017. See also arXiv:2310.07519**
- ★ In future works, we shall extend the analysis to all the **SPT-SZ clusters** (including those from SPTPol), redo the search with other search templates, using the observed radio emission as well as from dark matter annihilations.



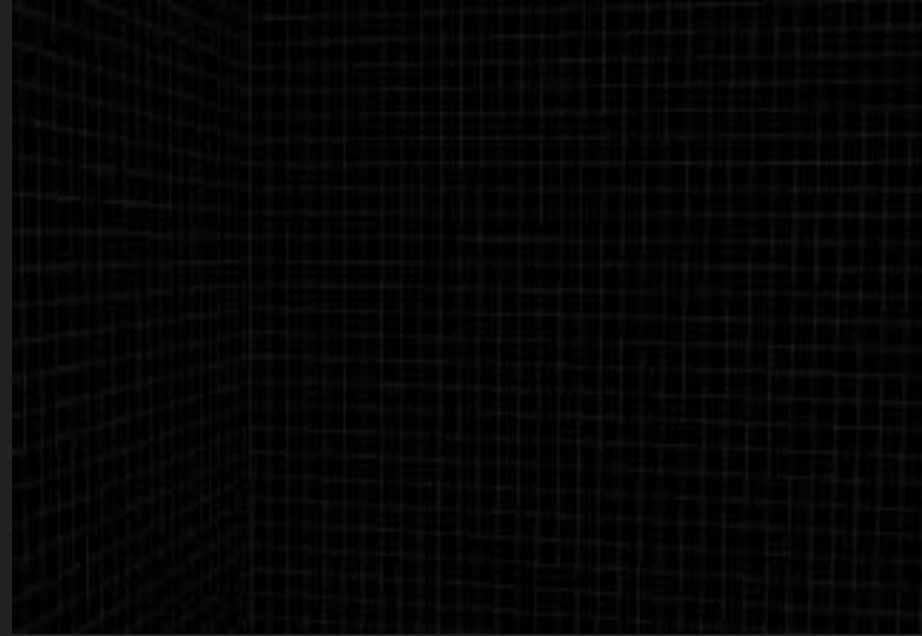
# MAXIMUM LIKELIHOOD ESTIMATION (MLE)

- ★ To analyze LAT data, **we construct the likelihood that is applicable to the LAT data, and then use this likelihood to find the best fit model parameters.** These parameters include the description of a source's spectrum, its position, and even whether it exists.
- ★ **Likelihood L is the probability of obtaining the data given an input model.** In our case, the input model is the distribution of gamma-ray sources on the sky, and includes their **intensity and spectra.**
- ★ Since we expect the best model to have the highest probability of resulting in the data, we **vary the spectral parameters until the likelihood is maximized.**
- ★ Test Statistic is defined as  **$TS = -2\ln(L_{max,0}/L_{max,1})$** , where  $L_{max,0}$  is the maximum likelihood value for a model without an additional source (the 'null hypothesis') and  $L_{max,1}$  is the maximum likelihood value for a model with the additional source at a specified location.
- ★ In the limit of a large number of counts, **Wilkes Theorem states that the TS for the null hypothesis is asymptotically distributed as  $\chi^2$  distribution.**
- ★ **Larger TS** indicates that the null hypothesis is incorrect (i.e., a **source really is present**), which can be quantified. As a basic rule of thumb, the square root of the TS is approximately equal to the detection significance for a given source.

# HOW ARE GAMMA RAYS PRODUCED IN GALAXY CLUSTERS



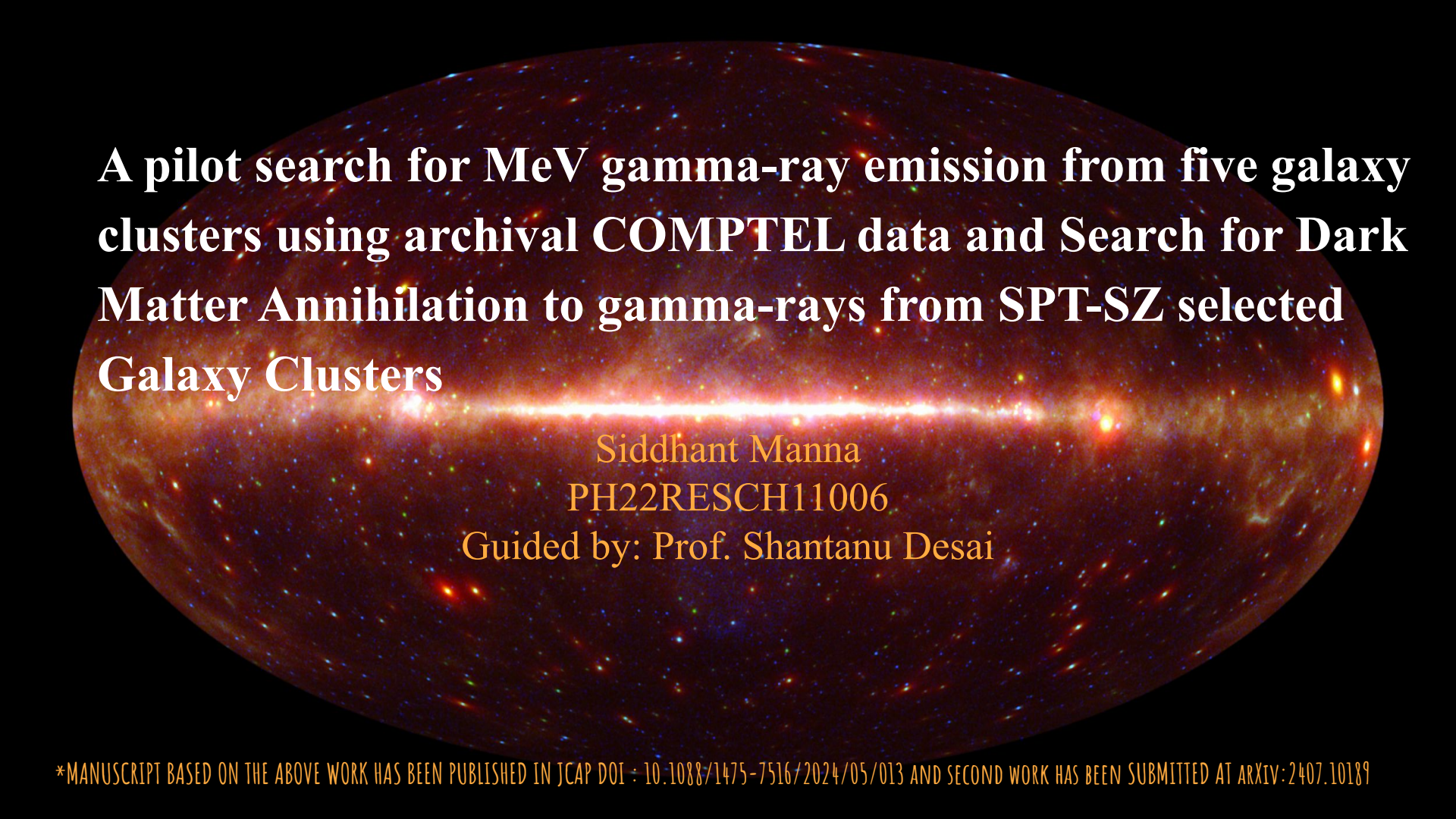
AGN'S



WIMP'S

# PREVIOUS SEARCHES WITH GAMMA-RAYS

- ★ Before the launch of the Fermi Gamma-ray Space Telescope, **O. Reimer et al. (2003)**, using **nine years of EGRET data** reported **upper limits for 58 X-ray-selected galaxy clusters for energies between 100 MeV- 30 GeV**.
- ★ **Dutson et al. (2013)** performed a search from **114 Brightest cluster galaxies (BCGs)** selected from multiple X-ray catalogs, using **45 months of Fermi-LAT data**. This search **detected signals from four possible sources**, although none of them could be unambiguously associated with the BCGs.
- ★ **Prokhorov et al. (2014)** using the **Fermi-LAT data above 10 GeV** did the **stacking of 55 clusters from the HIFLUGCS** sample. A **4.3 $\sigma$  excess** was obtained from this analysis, which was attributed to contribution from AGNs.
- ★ **Reiss et al. (2018)** did another **stacked search using 112 clusters in the MCXC catalogue** found evidence at **5.8 $\sigma$**  significance for a central point source dominated by AGN emission along with a gamma-ray ring at the position of the virial shock
- ★ A ring-like structure on the fringes of the **Coma galaxy cluster** was discovered using **eight years of Fermi-LAT data with 3.4 $\sigma$  significance** by **U. Keshet and I. Reiss (2018)**.
- ★ **Xi et al (2018)** confirmed the above detection using **nine years of Fermi-LAT data with the observed significance > 5 $\sigma$** .
- ★ No significant emission was seen from the VIRGO cluster, although emission was detected from two elliptical galaxies, M87 and M49 located near the **VIRGO center** by **Ackermann et al. (2018)**
- ★ **V. Baghmanyan et al. (2022)** reaffirmed the results and found **extended diffuse gamma-ray emission with 5.4 $\sigma$  significance based on 12.3 years of data**.
- ★ For our analysis, we are using the **SPT-SZ mass limited catalog** dataset to search for Gamma rays from Galaxy Clusters.



**A pilot search for MeV gamma-ray emission from five galaxy clusters using archival COMPTEL data and Search for Dark Matter Annihilation to gamma-rays from SPT-SZ selected Galaxy Clusters**

Siddhant Manna

PH22RESCH11006

Guided by: Prof. Shantanu Desai

Sunyaev &  
Zeldovich  
1980

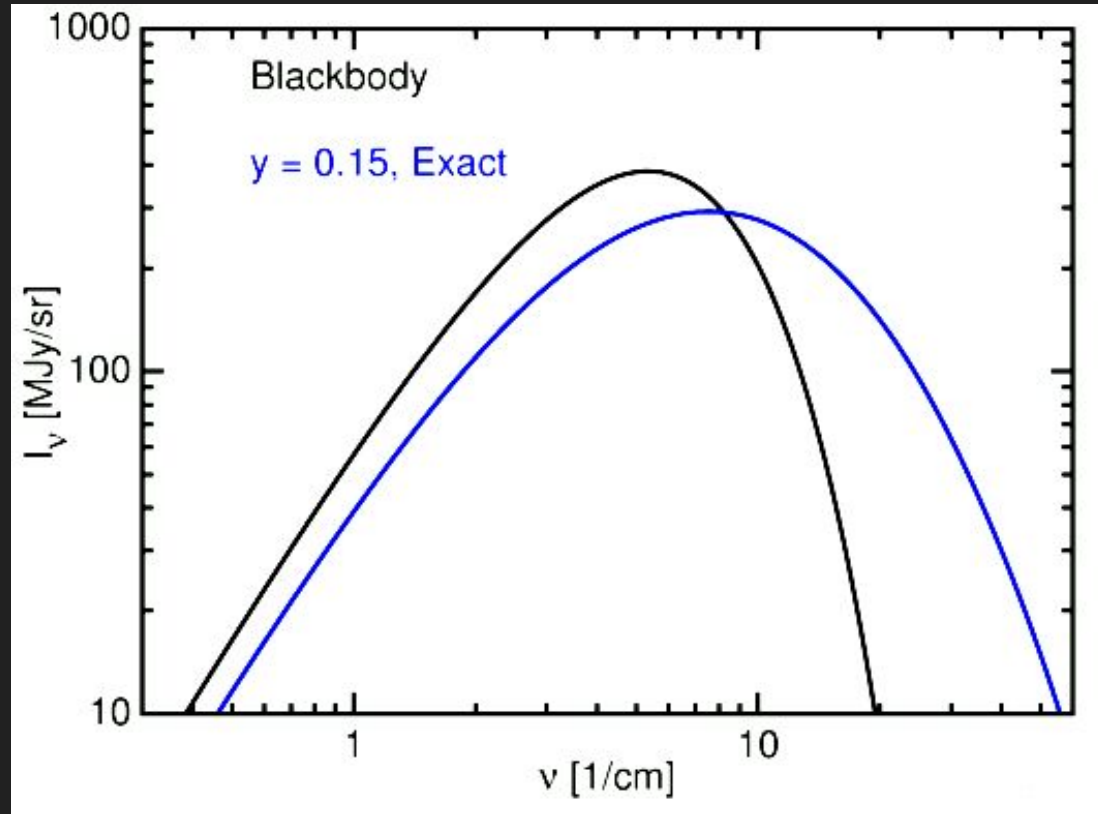
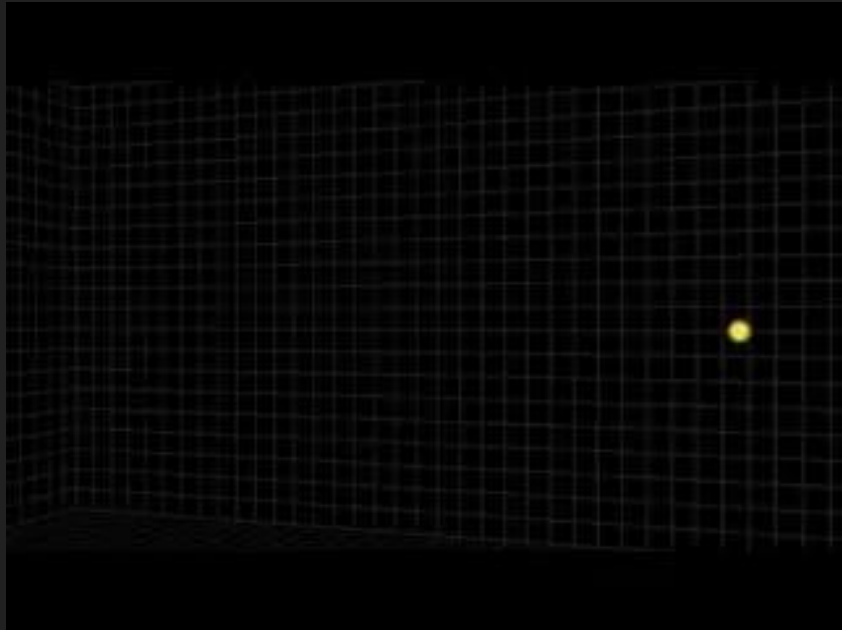
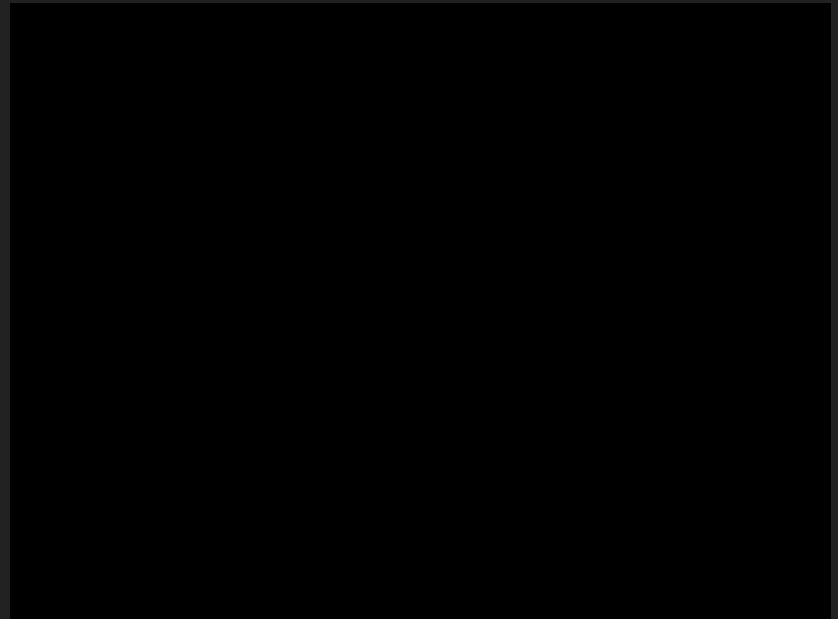


FIGURE SHOWS EFFECT OF COMPTON SCATTERING ON THE BLACKBODY SPECTRUM, UNDISTORTED (BLACK LINE) AND DISTORTED BY THE SUNYAEV-ZEL'DOVICH EFFECT (SZE) (BLUE LINE)

# How are gamma rays produced in galaxy clusters



INVERSE COMPTON SCATTERING



PION DECAY



- The first step in obtaining the halo concentration involves choosing a mass proxy. For this purpose, we use  $M_{200}$ , which is the **cluster mass at a spherical overdensity with a density 200 times the critical density of the Universe**. We have obtained  $M_{200}$  values from the **SPT-SZ 2500 square-degree catalogue**.
- **Virial radius,  $R_{200}$**  which can be estimated from  $M_{200}$  as follows:

$$R_{200} = (3M_{200}/4\pi\Delta_{200}\rho_{\text{crit}})^{1/3}$$

- where  $\Delta_{200}$  is the **overdensity factor**, which is 200 in this case. The critical density,  $\rho_{\text{crit}}$ , is calculated using the **Hubble parameter  $H(z)$** , which is the rate at which the universe expands.

$$\rho_{\text{crit}} = 3H^2(z) / 8\pi G$$

- No concentration measurements are available on a per cluster basis for the SPT sample. Therefore, we use the **concentration-mass (c – M ) relations** from cosmological simulations for modelling the dark matter halo.
- We use the c-M relation defined in [arXiv 1312.1729](#) by **M. A. Sánchez-Conde and F. Prada, 2014**, which have been shown to match the observation results across a wide range of halo masses, from dwarf spheroidal galaxies to galaxy cluster

- The **scale density**  $\rho_0$  can be computed from  $c_{200}$  as follows:

$$\rho_0 = \frac{2\Delta_{200}\rho_{\text{crit}}c_{200}}{3f(c_{200})}$$

- where  $f(c_{200})$  is given by:

$$f(c_{200}) = \frac{2}{c_{200}^2} \left[ \ln(1+c_{200}) - \frac{c_{200}}{1+c_{200}} \right]$$

# Analysis Process

Binned Fermi Analysis  
Process with template  
for potential dark matter  
annihilation emission  
modelled as diffuse  
source

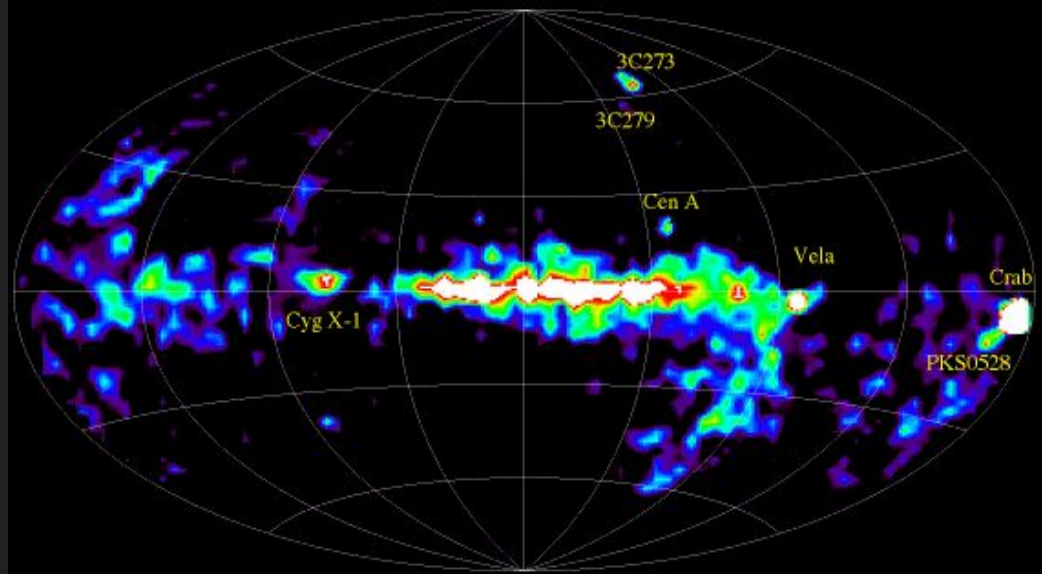


Halo and subhalo  
modelling as defined  
and calculating J-Factor  
values based on it.

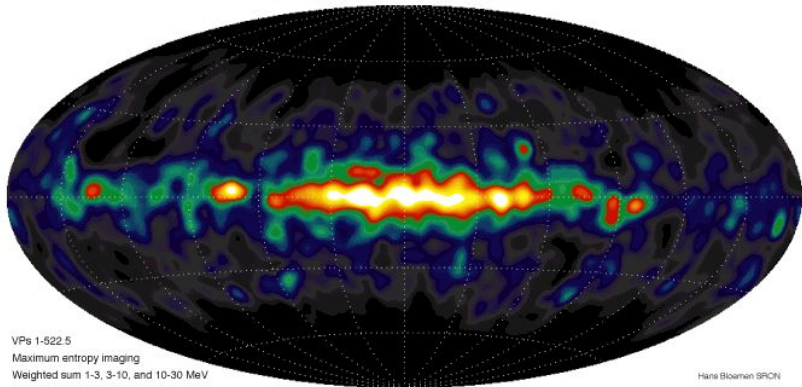
Likelihood Analysis and  
Test Statistic Values

## COMPTEL 1 to 30 MeV All-Sky Map

Credit: COMPTEL Collaboration



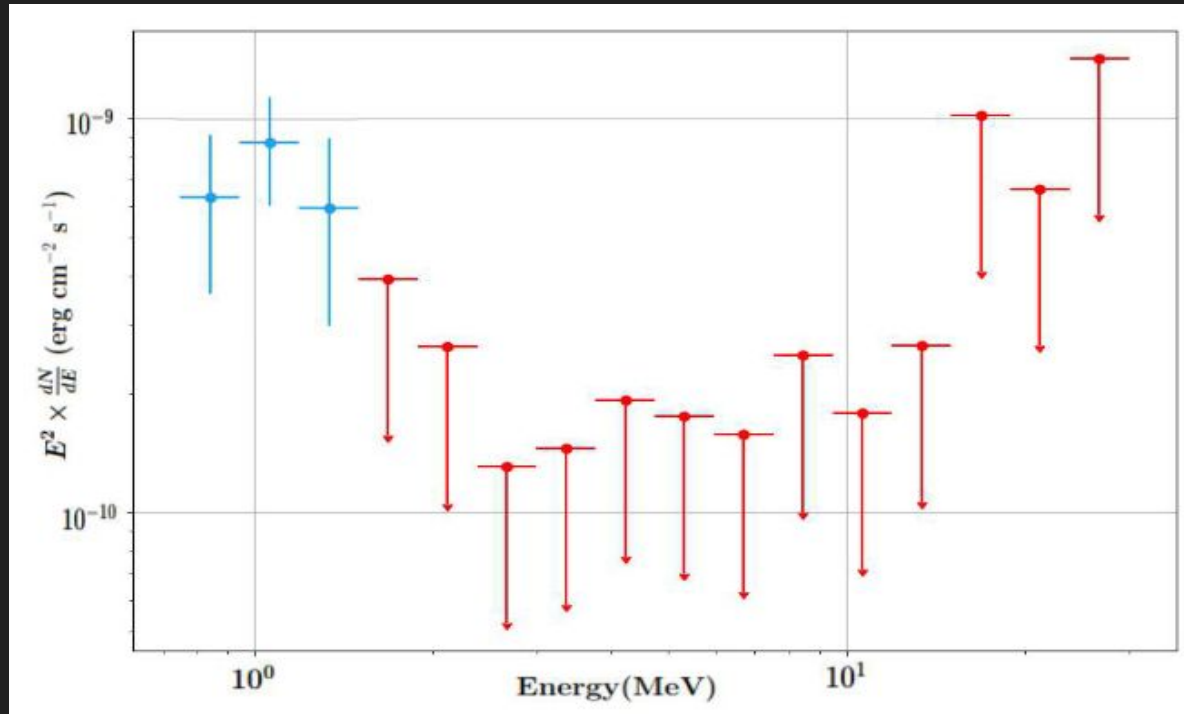
## COMPTEL 1-30 MeV



## COMPTEL 1 to 30 MeV Map of Milky Way

Credit: COMPTEL Collaboration

# RESULTS (SED Plots)

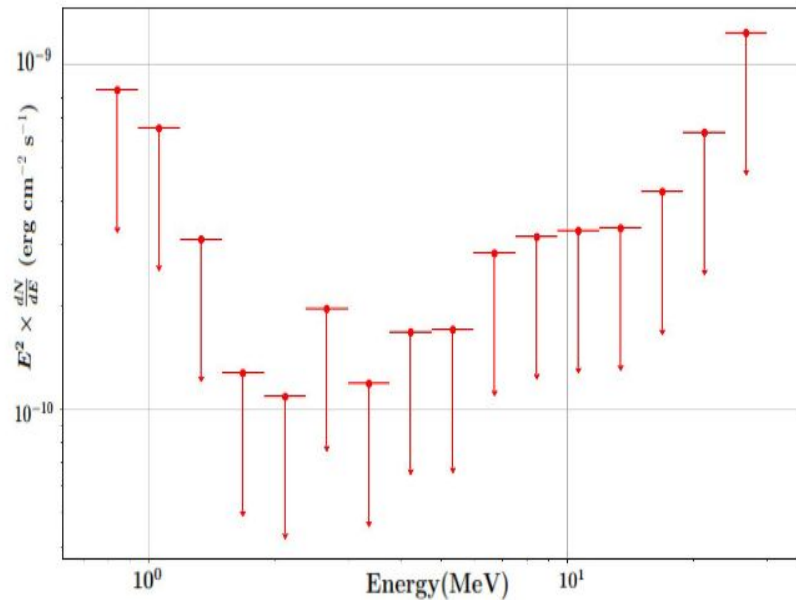


Similar to last figure but here the SED for VIRGO cluster is shown using Radial Gaussian source Template.

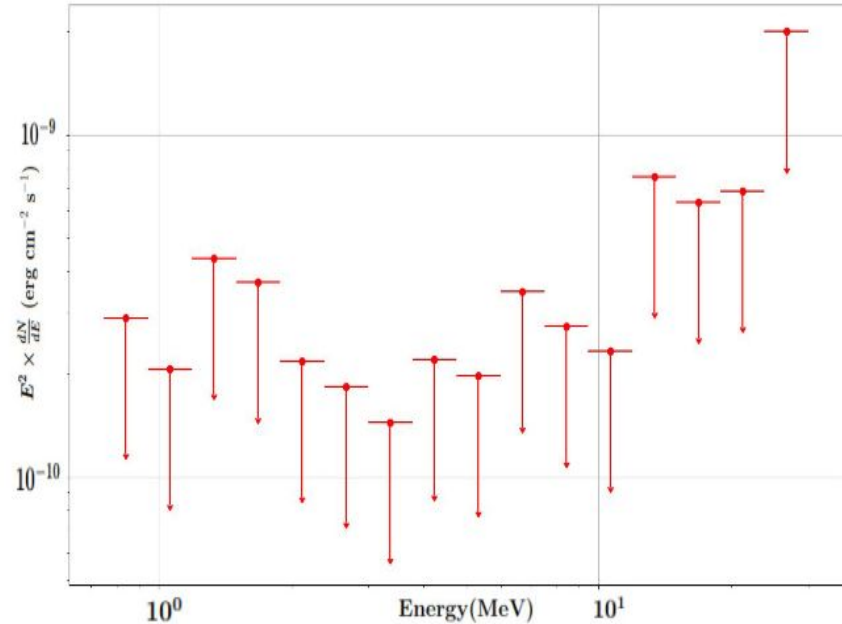
# CONCLUSIONS

- We report the **95% confidence level upper limits** for the differential photon flux (at 30 MeV), the integral photon flux, and photon energy flux.
- For Coma, SPT-CL J2012-5649, Bullet, and El Gordo, we report the **differential flux upper limit at 30 MeV, along with integral flux and energy flux upper limits**. For Coma cluster, the integral photon flux limit we obtain of about  $(1.4 - 1.5) \times 10^{-5} \text{ cm}^{-2}\text{s}^{-1}$  is comparable to the reported flux in *Iyudin et. al, 2004 (I04)*.
- All the remaining clusters with null results also show similar values for the differential and integral photon flux as well as the energy flux.
- For the **VIRGO cluster, we report the aforementioned measured quantities along with  $1\sigma$  error bars**, For the point source template, the total energy flux equals  $(0.57 \pm 0.25) \times 10^{-9} \text{ erg/cm}^2/\text{s}$ . When we use the radial disk and radial Gaussian templates, we get total photon energy fluxes of  $(1.25 \pm 0.48) \times 10^{-9} \text{ erg/cm}^2/\text{s}$  and  $(0.70 \pm 0.28) \times 10^{-9} \text{ erg/cm}^2/\text{s}$  respectively.
- Once again, the **photon flux is comparable to the  $^{16}\text{O}$  line flux reported in *Iyudin et al (2004)*, albeit measured at lower energies**. We note that the **AGN in M87 could be the cause of the observed MeV emission, since M87 has also been detected at very high energies**.
- **Our results have been published and are available at [arXiv:2401.13240](https://arxiv.org/abs/2401.13240) or [JCAP DOI](#)**

# RESULTS (SED Plots)

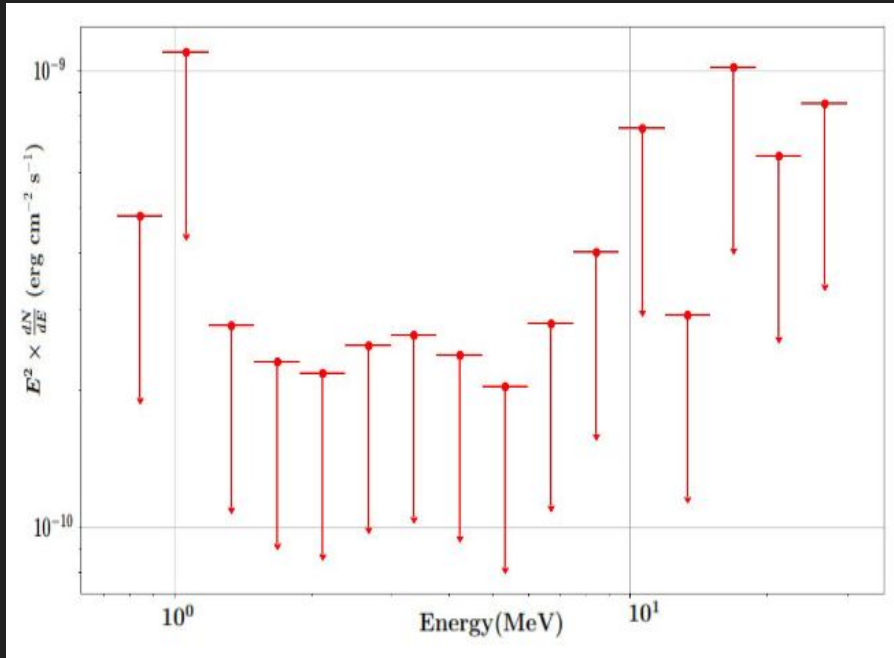


SED for Coma cluster using Point source Template

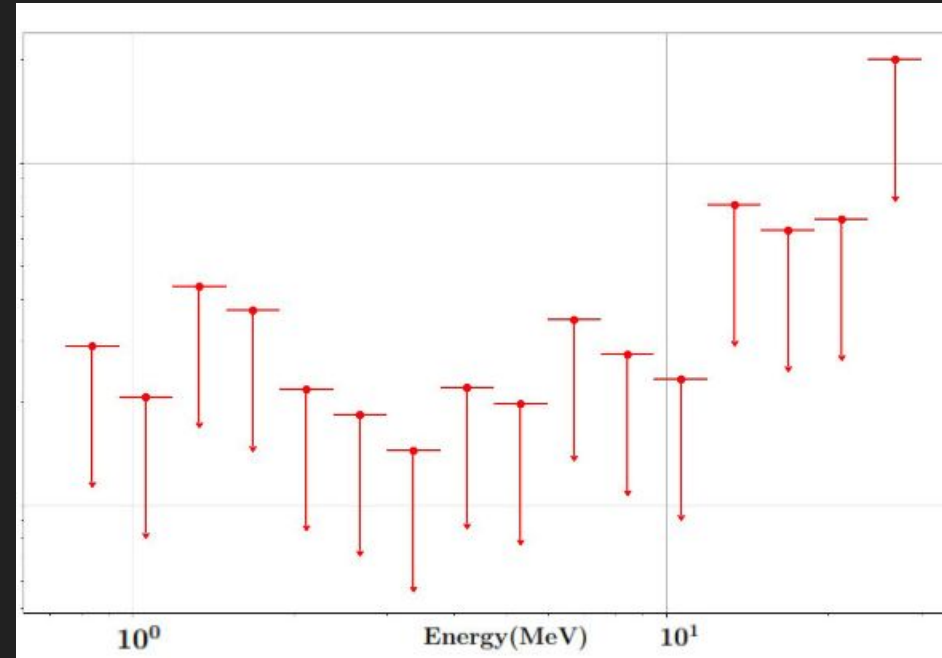


SED for SPT-CL J2012-5649 cluster using Point source Template

# RESULTS (SED Plots)



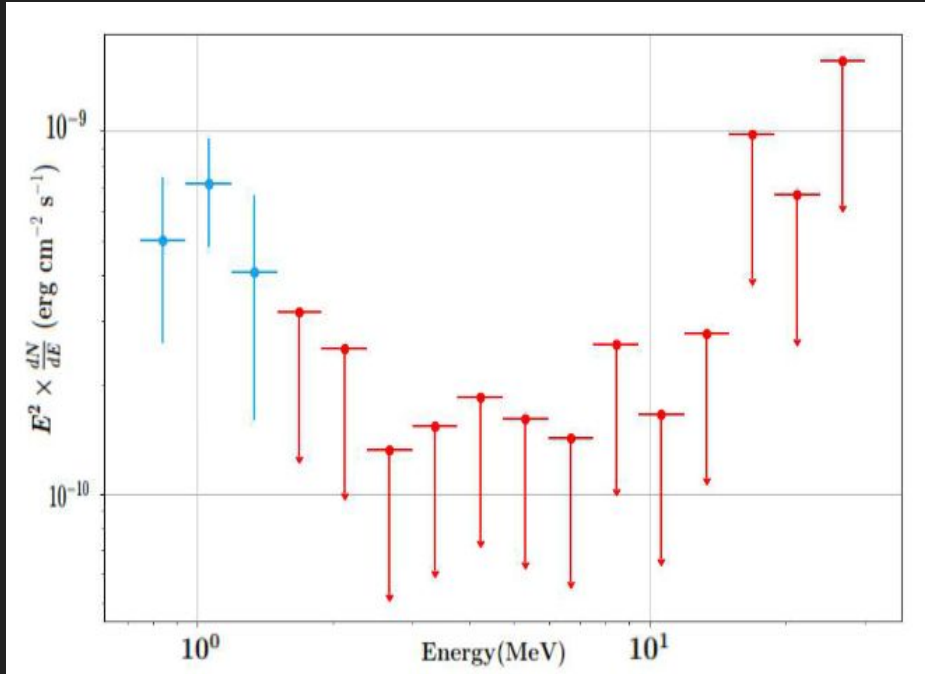
SED for El Gordo cluster using Point source Template



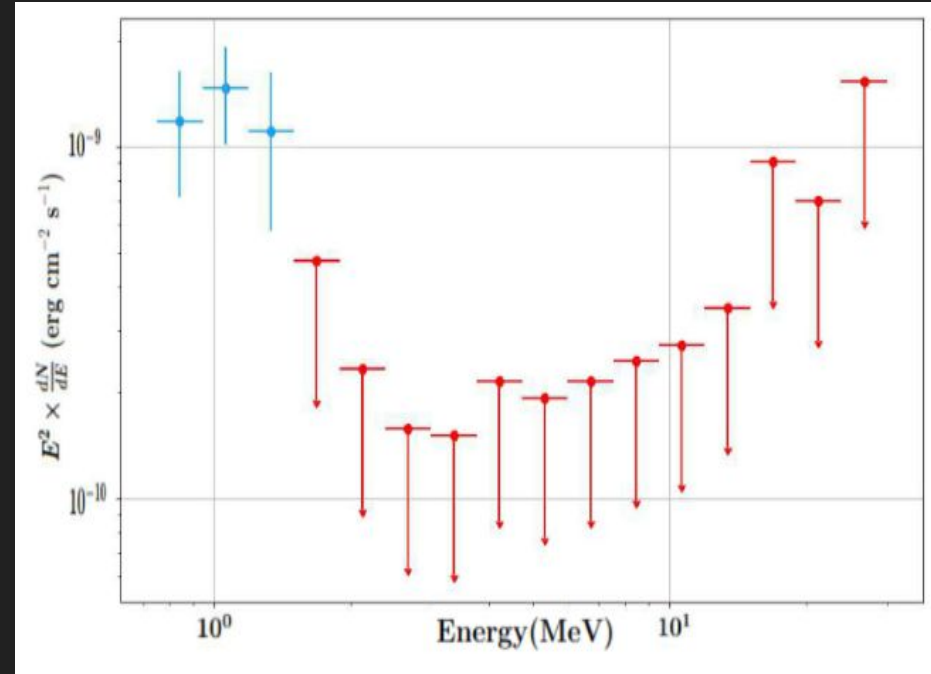
SED for Bullet cluster using Point source Template



# RESULTS (SED Plots)



SED for VIRGO cluster using Point source Template. The first three data points in blue show the measured non-zero flux, whereas those in red color at higher energies represent upper limits. The data points shown are the center of energy bins.



Similar to adjacent figure but here the SED for VIRGO cluster is shown using Radial Disk source Template.

Cluster Name	Template	Differential Flux (ph/cm <sup>2</sup> /s/MeV)	Integral Flux (ph/cm <sup>2</sup> /s)	Energy Flux (erg/cm <sup>2</sup> /s)
Coma	Point	$< 1.18 \times 10^{-8}$	$< 1.39 \times 10^{-5}$	$< 6.30 \times 10^{-11}$
	Radial disk	$< 1.31 \times 10^{-8}$	$< 1.54 \times 10^{-5}$	$< 6.98 \times 10^{-11}$
	Radial gaussian	$< 1.21 \times 10^{-8}$	$< 1.42 \times 10^{-5}$	$< 6.44 \times 10^{-11}$
SPT-CL J2012-5649	Point	$< 1.35 \times 10^{-8}$	$< 1.59 \times 10^{-5}$	$< 7.21 \times 10^{-11}$
	Radial disk	$< 1.70 \times 10^{-8}$	$< 1.98 \times 10^{-5}$	$< 9.03 \times 10^{-11}$
	Radial gaussian	$< 1.39 \times 10^{-8}$	$< 1.63 \times 10^{-5}$	$< 7.40 \times 10^{-11}$
Bullet	Point	$< 1.13 \times 10^{-8}$	$< 1.33 \times 10^{-5}$	$< 6.03 \times 10^{-11}$
	Radial disk	$< 1.32 \times 10^{-8}$	$< 1.55 \times 10^{-5}$	$< 7.04 \times 10^{-11}$
	Radial gaussian	$< 1.15 \times 10^{-8}$	$< 1.35 \times 10^{-5}$	$< 6.13 \times 10^{-11}$
El gordo	Point	$< 1.84 \times 10^{-8}$	$< 2.15 \times 10^{-5}$	$< 9.80 \times 10^{-11}$
	Radial disk	$< 1.97 \times 10^{-8}$	$< 2.33 \times 10^{-5}$	$< 9.94 \times 10^{-11}$
	Radial gaussian	$< 1.80 \times 10^{-8}$	$< 2.11 \times 10^{-5}$	$< 9.58 \times 10^{-11}$
Virgo	Point	$(0.35 \pm 0.21) \times 10^{-3}$	$(0.22 \pm 0.09) \times 10^{-5}$	$(0.57 \pm 0.25) \times 10^{-9}$
	Radial disk	$(0.75 \pm 0.40) \times 10^{-3}$	$(0.48 \pm 0.17) \times 10^{-5}$	$(1.25 \pm 0.48) \times 10^{-9}$
	Radial gaussian	$(0.42 \pm 0.24) \times 10^{-3}$	$(0.27 \pm 0.09) \times 10^{-5}$	$(0.70 \pm 0.28) \times 10^{-9}$

## RESULTS (TS VALUES AND EXPOSURE FOR ALL CLUSTERS AND TEMPLATES)

<b>Cluster Name</b>	<b>Template</b>	<b>TS Values</b>	<b>Exposure (cm<sup>2</sup> s)</b>
<b>Coma</b>	<b>Point</b>	<b>0.02</b>	<b>3.78 x 10<sup>9</sup></b>
	<b>Radial disk</b>	<b>0.06</b>	
	<b>Radial gaussian</b>	<b>0.01</b>	
<b>SPT-CL J2012-5649</b>	<b>Point</b>	<b>1.44</b>	<b>0.84 x 10<sup>9</sup></b>
	<b>Radial disk</b>	<b>2.74</b>	
	<b>Radial gaussian</b>	<b>1.90</b>	
<b>Bullet</b>	<b>Point</b>	<b>0.00</b>	<b>3.94 x 10<sup>9</sup></b>
	<b>Radial disk</b>	<b>0.00</b>	
	<b>Radial gaussian</b>	<b>0.00</b>	
<b>El gordo</b>	<b>Point</b>	<b>1.12</b>	<b>1.74 x 10<sup>9</sup></b>
	<b>Radial disk</b>	<b>2.40</b>	
	<b>Radial gaussian</b>	<b>1.00</b>	
<b>Virgo</b>	<b>Point</b>	<b>3.00</b>	<b>1.12 x 10<sup>9</sup></b>
	<b>Radial disk</b>	<b>5.60</b>	
	<b>Radial gaussian</b>	<b>3.60</b>	